NAVAL POSTGRADUATE SCHOOL
MONTEREY, CALIFORNIA

THESIS

COMPARISON OF EVAPORATION DUCT
HEIGHT MEASUREMENT METHODS AND
THEIR IMPACT ON RADAR PROPAGATION
ESTIMATES

by

John David Whalen

March 1998

Thesis Advisor: Kenneth L. Davidson

Approved for public release; distribution is unlimited.

REPORT DOCUMENTATION PAGE		Form Approved OMB No. 0704-0188

Public reporting burden for this collection of information is estimated to average 1 hour per response, including the time for reviewing instruction, searching existing data sources, gathering and maintaining the data needed, and completing and reviewing the collection of information. Send comments regarding this burden estimate or any other aspect of this collection of information, including suggestions for reducing this burden, to Washington Headquarters Services, Directorate for Information Operations and Reports, 1215 Jefferson Davis Highway, Suite 1204, Arlington, VA 22202-4302, and to the Office of Management and Budget, Paperwork Reduction Project (0704-0188) Washington DC 20503.

1. AGENCY USE ONLY *(Leave blank)*	2. REPORT DATE March 1998	3. REPORT TYPE AND DATES COVERED Master's Thesis	
4. TITLE AND SUBTITLE COMPARISON OF EVAPORATION DUCT HEIGHT MEASUREMENT METHODS AND THEIR IMPACT ON RADAR PROPAGATION ESTIMATES		5. FUNDING NUMBERS	
6. AUTHOR John David Whalen			
7. PERFORMING ORGANIZATION NAME(S) AND ADDRESS(ES) Naval Postgraduate School Monterey CA 93943-5000		8. PERFORMING ORGANIZATION REPORT NUMBER	
9. SPONSORING/MONITORING AGENCY NAME(S) AND ADDRESS(ES)		10. SPONSORING/MONITORING AGENCY REPORT NUMBER	

11. SUPPLEMENTARY NOTES The views expressed in this thesis are those of the author and do not reflect the official policy or position of the Department of Defense or the U.S. Government.

12a. DISTRIBUTION/AVAILABILITY STATEMENT Approved for public release; distribution is unlimited.	12b. DISTRIBUTION CODE

13. ABSTRACT *(maximum 200 words)*

    A study was performed to compare shipboard measurements of atmospheric parameters that impact the evaporation duct and its effect on the propagation of electromagnetic energy from the AEGIS AN/SPY-1 radars. Two ships, USS ANZIO and USS CAPE ST GEORGE, participated in the annual NATO exercise, BALTOPS, during the summer of 1997. They were equipped with an automated METOC sensor system, developed by John Hopkins University Applied Physics Laboratory, called SEAWASP. SEAWASP provided continuous measurement of parameters determining near surface refractivity and the evaporative duct throughout the cruise. SEAWASP data were compared with manual bridge observations in order to illustrate the difference in propagation conditions assessed by the two methods. Additionally, ERS-1 Scatterometer wind data were used in conjunction with SEAWASP data to determine the feasibility of incorporating satellite wind data in determining evaporative duct heights. The automated SEAWASP data was able to depict, with greater accuracy, the constantly changing duct height conditions whereas the bridge observations, made at hourly intervals, lacked temporal resolution, thereby missing much of the variation in duct height. The discrepancies in duct heights between the two measurement systems led to differing propagation ranges resulting in shorter reaction times to counter threats to the ship.

14. SUBJECT TERMS Environmental Data, Radio Physical Optics, Radar Performance Prediction, Refraction, Evaporative Duct, Engineer's Refractive Effects Prediction System			15. NUMBER OF PAGES 75
			16. PRICE CODE
17. SECURITY CLASSIFICATION OF REPORT Unclassified	18. SECURITY CLASSIFICATION OF THIS PAGE Unclassified	19. SECURITY CLASSIFICATION OF ABSTRACT Unclassified	20. LIMITATION OF ABSTRACT UL

NSN 7540-01-280-5500 Standard Form 298 (Rev. 2-89)
Prescribed by ANSI Std. 239-18 298-102

COMPARISON OF EVAPORATION DUCT HEIGHT MEASUREMENT METHODS AND THEIR IMPACT ON RADAR PROPAGATION ESTIMATES

John David Whalen
Lieutenant Commander, United States Navy
B.S., United States Naval Academy, 1985

Submitted in partial fulfillment
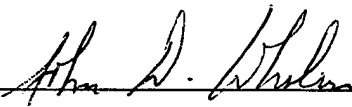of the requirements for the degree of

MASTER OF SCIENCE IN METEOROLOGY AND PHYSICAL OCEANOGRAPHY

from the
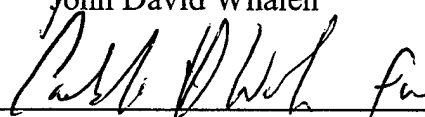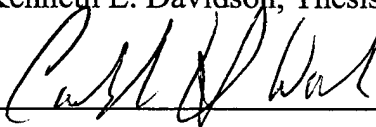
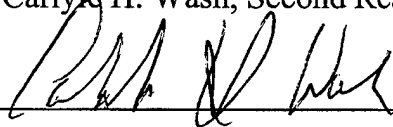## NAVAL POSTGRADUATE SCHOOL
March 1998

Author:_____

John David Whalen

Approved by:_____

Kenneth L. Davidson, Thesis Advisor

_____

Carlyle H. Wash, Second Reader

_____

Carlyle H. Wash, Chairman
Department of Meteorology

ABSTRACT

A study was performed to compare shipboard measurements of atmospheric parameters that impact the evaporation duct and its effect on the propagation of electromagnetic energy from the AEGIS AN/SPY-1 radars. Two ships, USS ANZIO and USS CAPE ST GEORGE, participated in the annual NATO exercise, BALTOPS, during the summer of 1997. They were equipped with an automated METOC sensor system, developed by John Hopkins University Applied Physics Laboratory, called SEAWASP. SEAWASP provided continuous measurement of parameters determining near surface refractivity and the evaporative duct throughout the cruise. SEAWASP data were compared with manual bridge observations in order to illustrate the difference in propagation conditions assessed by the two methods. Additionally, ERS-1 Scatterometer wind data were used in conjunction with SEAWASP data to determine the feasibility of incorporating satellite wind data in determining evaporative duct heights. The automated SEAWASP data was able to depict, with greater accuracy, the constantly changing duct height conditions whereas the bridge observations, made at hourly intervals, lacked temporal resolution thereby missing much of the variation in duct height. The discrepancies in duct heights between the two measurement systems led to differing propagation ranges resulting in shorter reaction times to counter threats to the ship.

TABLE OF CONTENTS

I. INTRODUCTION

The transition of naval warfare from the open ocean to the littoral region coupled with enhanced sophistication in weapons and sensors has increased the importance of environmental effects in the conduct of naval operations. Due to near shore operations, air defense capabilities are threatened by low radar cross section, low-altitude, high-speed cruise missiles launched from shore installations. These missiles have created a small window of opportunity for detection and reaction against this threat. To combat this, air defense sensors were developed with greater power and sensitivity. However, this created the side effect of significant environmental impact on sensor performance. The major environmental factors of concern are wind, temperature, relative humidity and local weather that influence the electromagnetic or refractivity conditions encountered by a ship's radar sensors.

The current methods of collecting these data using rocketsondes, rawinsondes, and bridge observations are time consuming and, in the case of a littoral region, unavailable due to restricted territorial seas. The overall result is to reduce the ability to sense environmental data beyond the local area. Additionally, environmental data can change rapidly along the coastal zone, especially during the transition from day to night. This can significantly impact propagation effects from a ships radar. Real time data collection and input into a weapon systems are also hampered due to the manual adjustments required to interpret and subsequently process the data for incorporation into that weapon system. The requirement of an accurate and real-time understanding of the constantly changing electromagnetic environment in the near-shore region is critical.

The AEGIS Program Office (PMS400) recognized the critical impact of the changing environment on ship self-defense. Figure 1.1 from PMS-400 illustrates results from both observations and predictions during at-sea exercises and show the value of including atmospheric influences for tracking low-flying targets. Specifically it shows how important in situ measurements are for determining firm track ranges. The dashed line represents a 4/3 earth or nominal horizon while the solid line represents a missile trajectory profile. When the ship has accurate in situ atmospheric measurements available, it can extend its ability to determine a firm track range 25nm beyond the 4/3 earth horizon. Assuming a target velocity of 600 knots, this equates to almost 2.5 minutes of increased detection time available to the warfare commander. Figure 1.1 demonstrates that the predicted ranges based on accurate environmental data are validated by observations. For purposes of this thesis, the assumption of mach one (600 knots or 1nm=6secs) for missile speed was used in all calculations. The 4/3's earth horizon applies for a standard atmosphere which would be used if in situ data were not available or not taken into account. It is important to determine if track ranges determined with surface measurements are better than having no data or non-representative data.

This demonstrated importance of knowing atmospheric conditions motivated the AEGIS program office (PMS-400) to fund John Hopkins University/Applied Physics Laboratory (JHU/APL) to develop an environmental sensor and acquisition system that will assist a ship's radar controller in configuring in real-time the AN/SPY-1 radar for optimal performance under existing environmental conditions. This sensor/acquisition system is called SEAWASP (Shipboard Environmental Assessment/Weapon System Performance) and

2

is the first step in providing automated, continuous, environmental data for real-time AN/SPY-1 performance estimates. Measurements are made from two shipboard meteorological masts and when needed, rocketsondes and floatsondes. Data from these measurements are then used in environmental models for determining refractivity conditions for the local area. It should be noted that the evaporation duct height cannot be determined operationally by rawinsondes or from multi-level fixed measurements because the surface gradients occur over heights that are too low to measure.

While SEAWASP can fulfill the requirement for the local operation area of the ship, future requirements will address the measurement of environmental factors contributing to the ship's down range radar propagation. To address this, remote sensing techniques must be used as well as in situ measurements from manned and unmanned aircraft resources.

This thesis will examine the impact of predicting radar propagation conditions using SEAWASP versus the observation procedures currently employed on naval ships. The data examined came from a two month cruise of two AEGIS class ships from Norfolk, VA to the Baltic Sea and their return during the summer of 1997. The examination will also address satellite remote sensing capabilities to estimate wind which influences propagation conditions. This will be done by comparing ERS-2 scatterometer derived surface winds with those recorded by SEAWASP and manual observation. While winds alone cannot determine ducting conditions, they can be an important factor under certain conditions. This examination of remote sensing solutions to this observation problem is viewed as a beginning of future research in this area.

Predicted vs Actual Firm Track Range

x = Observed firm track range
+ = Predicted firm track range

Predicted 4/3
Earth firm
track range

4/3 Earth
horizon

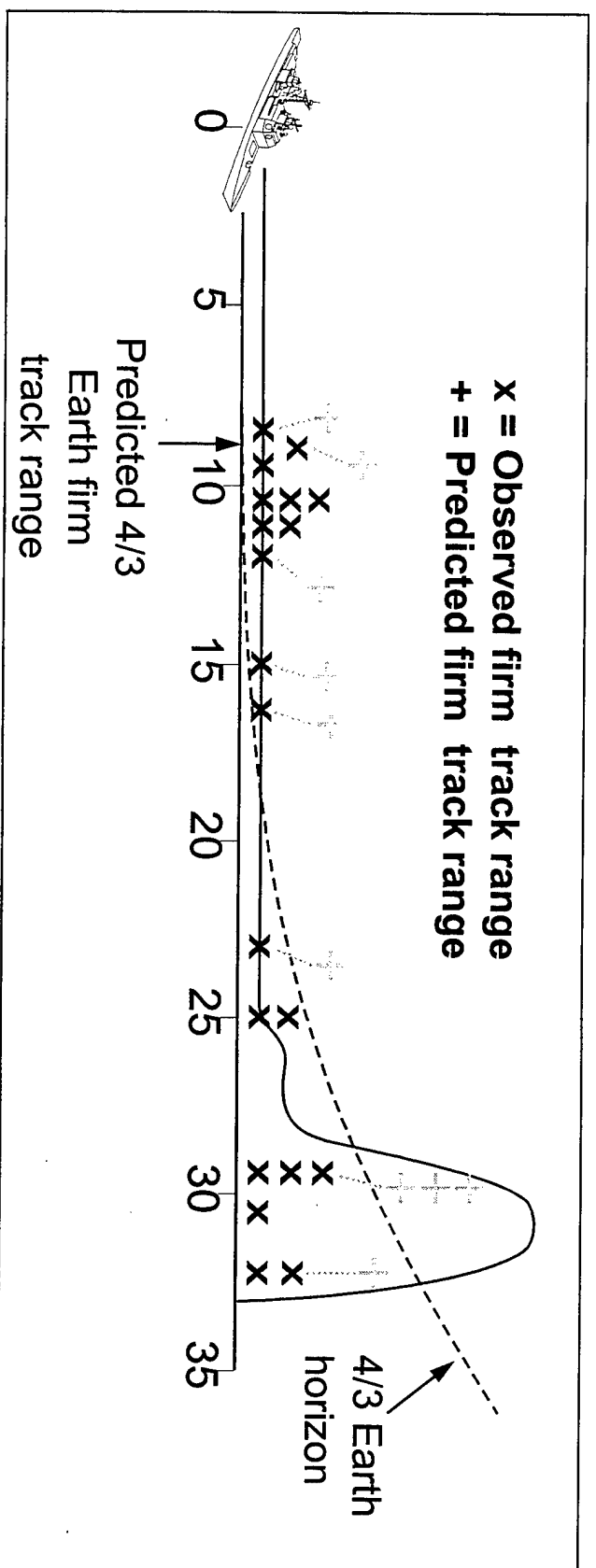0   5   10   15   20   25   30   35

Figure 1.1 Predicted vs Actual Firm Track Range. Predicted firm track range calculated from   environmental measurements taken by instrumented helicopter. (AEGIS Program Office, 1997)

II. BACKGROUND

A. PURPOSE

The Navy (Dalton, 1994) has described the shift of Naval operations from the "blue" or open ocean warfare to the smaller littoral regions. This transition to littoral warfare presents a significantly different problem to the warfare commander because of ship's vulnerability to smaller, more difficult to detect targets in a region where rapid environmental changes occur.

Current Navy tactical guidelines from the Surface Warfare Development Group define the need for understanding and using the environment in which naval forces operate:

To adequately define expected detection ranges for a given threat, an accurate assessment of the environment and its impact on sensor systems and employment is required. Depending on the environmental conditions being experienced, system performance could be enhanced or degraded. The primary environmental factors which impact detection ranges are temperature, atmospheric pressure, relative humidity, and local weather. The operating environment (e.g. near land/overland, littoral, or open ocean) also effects ranges. (COMSURFWARDEVGRU TACMEMO, Mar 95)

Accurate, continuous surface layer measurements are needed for reliable refractive assessment. Environmental conditions change rapidly (both spatially and temporally) in the coastal region. An example is the sea/shore interface during the transition from night to day. In most cases, whatever environmental data and forecasts are available must be studied by

the radar operator who then makes manual adjustments following a trial and error process. This leads to valuable time lost in a warfare situation where time is critical for defense of friendly operating forces.

The Oceanographer of the Navy (Clarke, 1997) has described the impact of environmental assessment in view of present and future emphasis. The new emphasis on exploiting in situ measurements to support weapons systems performance prediction is called Rapid Environmental Assessment (REA). Local measurements and nowcasting are important cornerstones of REA, replacing reliance on remote center numerical forecasting.

Ship self-defense is critical in the littoral region and requires almost instant adjustments to weapons and sensors to combat the difficult threats. Examples include low-altitude, high-speed cruise missiles in the evaporative duct and the exo-atmospheric threat of Tactical Ballistic Missiles (Lockheed Martin, 1996). The low Radar Cross Section (RCS) and flight profiles of low-altitude, high-speed Anti-Ship Cruise Missiles (ASCM) provide a limited capability for radar sensors to detect and engage these targets. To counter this threat air defense sensors were designed with higher power and greater sensitivity to detect the smaller targets. However, this came with a significant increase in the role the local environment had on the radar's effectiveness . With the radar's increased power and sensitivity at longer ranges, atmospheric effects produce anomalies in range accuracy, enhance signal attenuation, and produce more clutter. All of this leads to additional track loading and radar search time that ultimately decreases the tactical effectiveness of ship's radar system. Additionally, atmospheric effects can cause dual tracks that can confuse the radar controller. This can directly lead to a shortening of reaction time against a high-speed

threat, thus reducing the odds of a successful defensive engagement.

The increased awareness of the local environment on naval operations led to a system called SEAWASP (Shipboard Environmental Assessment/WeApon System Performance) fulfilling a requirement from the AEGIS program office. The AEGIS program office tasked John Hopkins University Applied/Physics Laboratory (JHU/APL) to develop an automated shipboard sensor system to detect and process the environmental parameters affecting radar propagation. The system also has to disseminate this information directly into the AEGIS weapon/sensor system for automatic adjustments to achieve enhanced radar performance in a rapidly changing environment.

B.   SEAWASP DESCRIPTION

SEAWASP consists of an environmental assessment subsystem and a radar assessment subsystem. SEAWASP radar performance assessments are based on depictions of atmospheric refractivity profiles obtained by its environmental assessment subsystem from measurements of deck-mounted sensors (met masts), rocketsondes, and floatsondes. The met masts are located on the port and starboard sides of the aft VLS (Vertical Launch System) deck (Fig. 2.1). Two masts are needed to enhance the probability that uncorrupted measurements can made at any time given the ship's own movement. The masts are mounted at approximately 9m above the sea surface. The sensors measure wind speed and direction, air temperature, sea temperature, barometric pressure, and relative humidity (Fig. 2.2&2.3). The sensor's measurements are used to depict atmospheric phenomena that impact AN/SPY-1's tracking performance for low altitude targets (SEAWASP User Guide, 1997). These phenomena include evaporative ducts, surface-based ducts, subrefraction, and low

7

altitude elevated ducts.   The resulting refractivity profiles are used to calculate RF propagation factor for AN/SPY-1 parameters. Propagation factor defines the atmosphere's effect on the distribution of radar energy with altitude and range, thus impacting probability of detection.

SEAWASP uses the TEMPER propagation model to calculate propagation factor. TEMPER accounts for AN/SPY-1's frequency, polarization, antenna height, and radiation patterns as well as the refractivity conditions. TEMPER calculates the propagation factor based on refractivity profiles from the environmental assessment subsystem. Ultimately TEMPER will be replaced by the Navy standard propagation model, the RPO (Radio Physical Optics) model.

Once SEAWASP is initialized, the met mast's sensors start to continuously sample the environment and send these data to the environmental data processor which then calculates the evaporation duct conditions. SEAWASP usually generates a new assessment of refractivity conditions every five minutes. Evaporative ducting is the most pervasive refractive effect over the ocean and is result of a rapid decrease in humidity just above the sea surface. Evaporative duct conditions can be estimated from time averages of air and sea temperatures, humidity, and wind speed. Additionally, SEAWASP can request deployment of a floatsonde to improve the evaporative duct estimate.

While not discussed in this thesis, SEAWASP can also attempt to depict surface-based ducting, caused by low level temperature inversions.   In order to accurately depict such a duct, a rocketsonde is needed to make upper level refractivity profile. SEAWASP can, based on Met Mast data, make requests for such rocketsondes if it detects the possibility

of such a duct.

Once the environmental data processor produces a refractivity profile, this profile is passed to the radar performance assessment subsystem which automatically obtains AN/SPY-1 settings from the Combat Display and Control System (CDCS). SEAWASP then calculates and displays probabilities of detection under the existing refractive conditions.

Shipboard use of SEAWASP began in 1993 consisting of periodic testing aboard AEGIS cruisers until SEAWASP was installed on CG-68 and CG-71 in 1994. The current version of SEAWASP installed on these ships is the first fully autonomous version and is the focus of this thesis. Previous to this cruise, SEAWASP has undergone extensive field testing in such diverse areas such diverse as Puerto Rico, the Mid-Atlantic, Hawaii and the Arabian Gulf (Konstanzer, 1996). Additionally, before and after each evaluation cruise SEAWASP's calibration is checked to ensure accuracy. This thorough testing and evaluation by JHU/APL and the AEGIS program office has validated SEAWASP to be an accurate, autonomous sensor. For purposes of this thesis, SEAWASP is considered to be highly accurate.

C.   SCATTEROMETER DATA

This thesis also evaluates, at least initially, the ability to incorporate satellite data, ERS-2 scatterometer, into the evaporation duct calculation process. The scatterometer only provides spatial information on the surface wind. Wind is not the primary parameter but is an important parameter in determining the occurance of surface ducting conditions. This is because it impacts mixing in the near surface layer. Satellite information, in general, is valuable because it will become important for a commander to assess ducting conditions

9

away from the ship. SEAWASP addresses those refractive conditions in the local area of the ship but knowledge of what is happening over the horizon is also of importance as weapons extend to greater and greater ranges. While the ERS-2 only provides a part of the data needed to determine refractivity conditions, further study and validation of other satellite derived products may culminate in the ability to use satellite data to predict and measure refractivity conditions over the horizon.

This thesis is based on operational conditions and data occurring with a cruise in the summer of 1997 during which the USS ANZIO (CG-68) and USS CAPE ST GEORGE (CG-71) were outfitted with SEAWASP for the annual Baltic exercise BALTOPS '97. Both ships, home-ported in Norfolk, VA, sailed in late May 1997 and returned in late July 1997, spending most of the cruise in the Baltic Sea and in port. There were two key measurement periods, the transit from and to Norfolk across the North Atlantic and the period covering operations in the Baltic Sea. At different periods of the cruise the SEAWASP system was sometimes turned off neccessitating the need to treat both ships as one platform when comparing the SEAWASP data versus that collected by bridge personnel (i.e. this is not a comparison of ship vs ship).
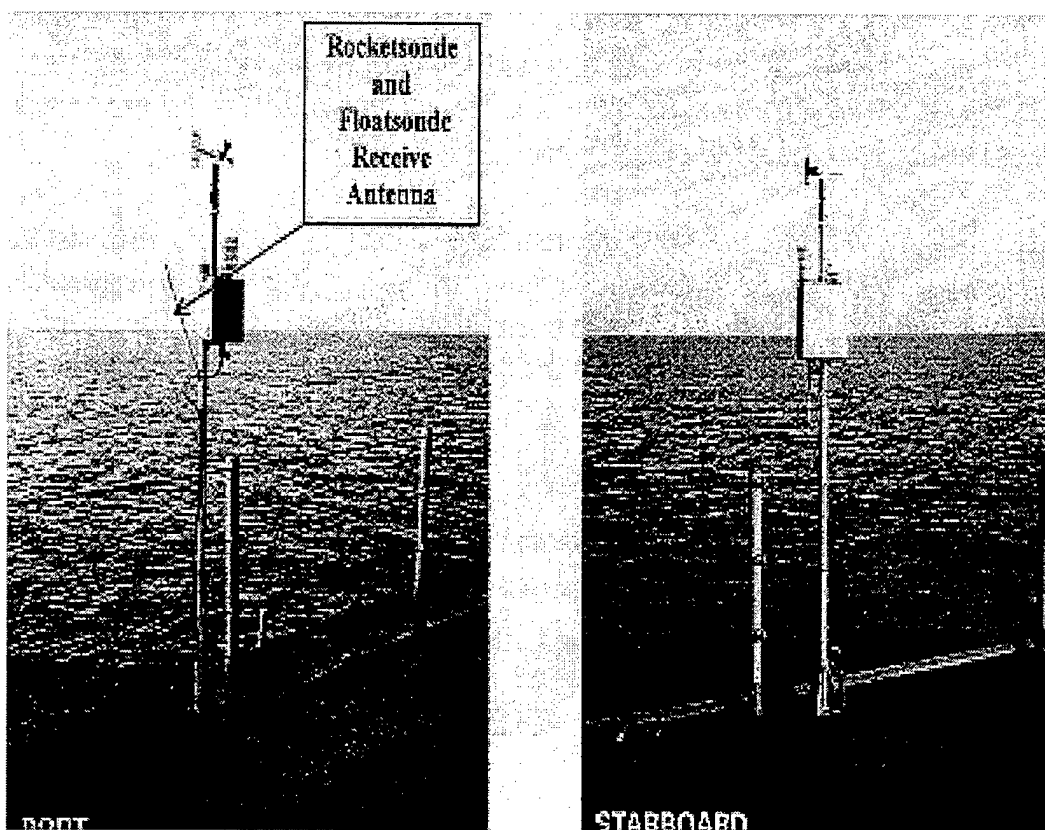
Figure 2.1 SEAWSP Met Masts. View of the port and starboard Met Masts on the VLS deck, 9m above surface of the water.
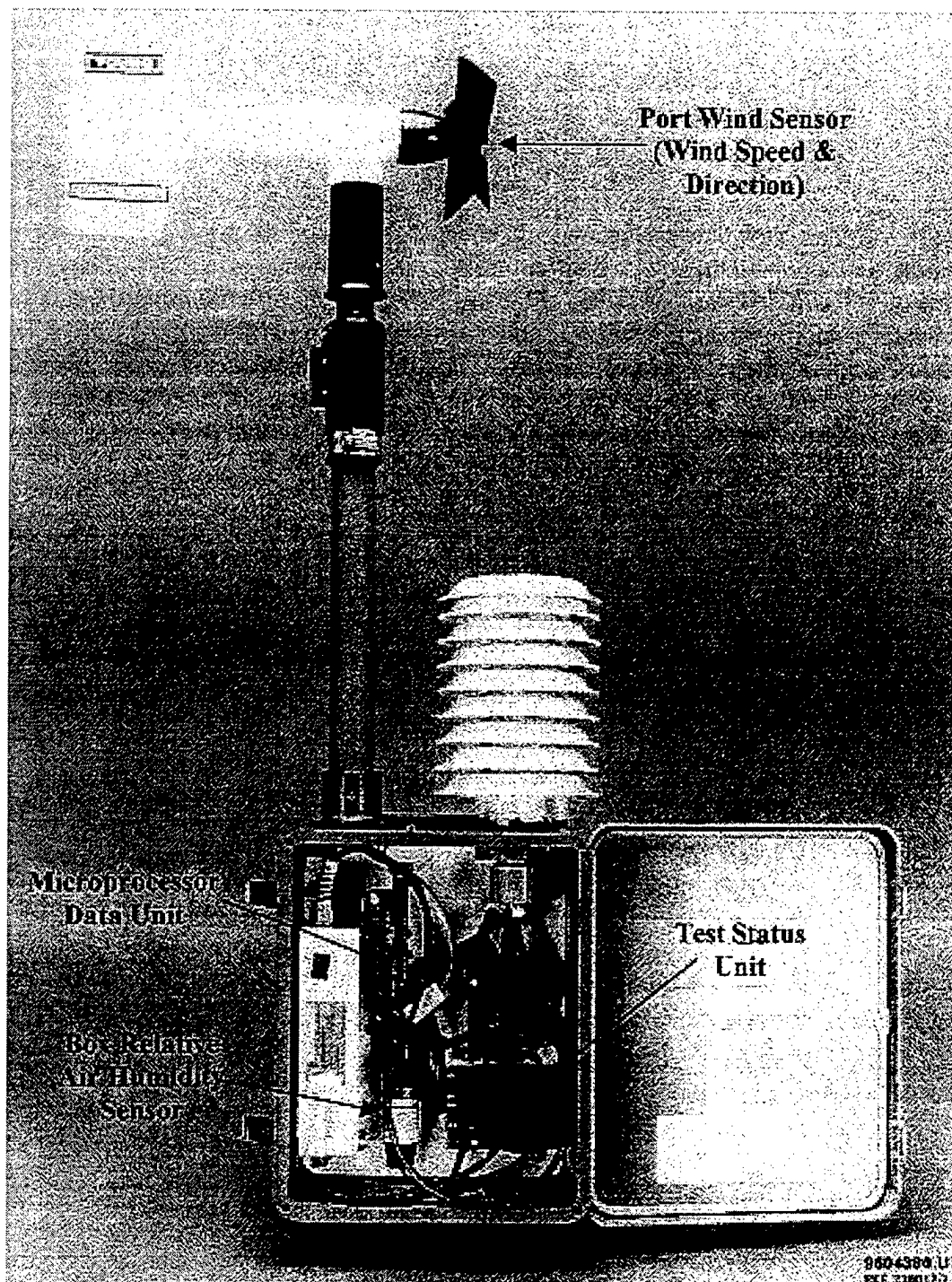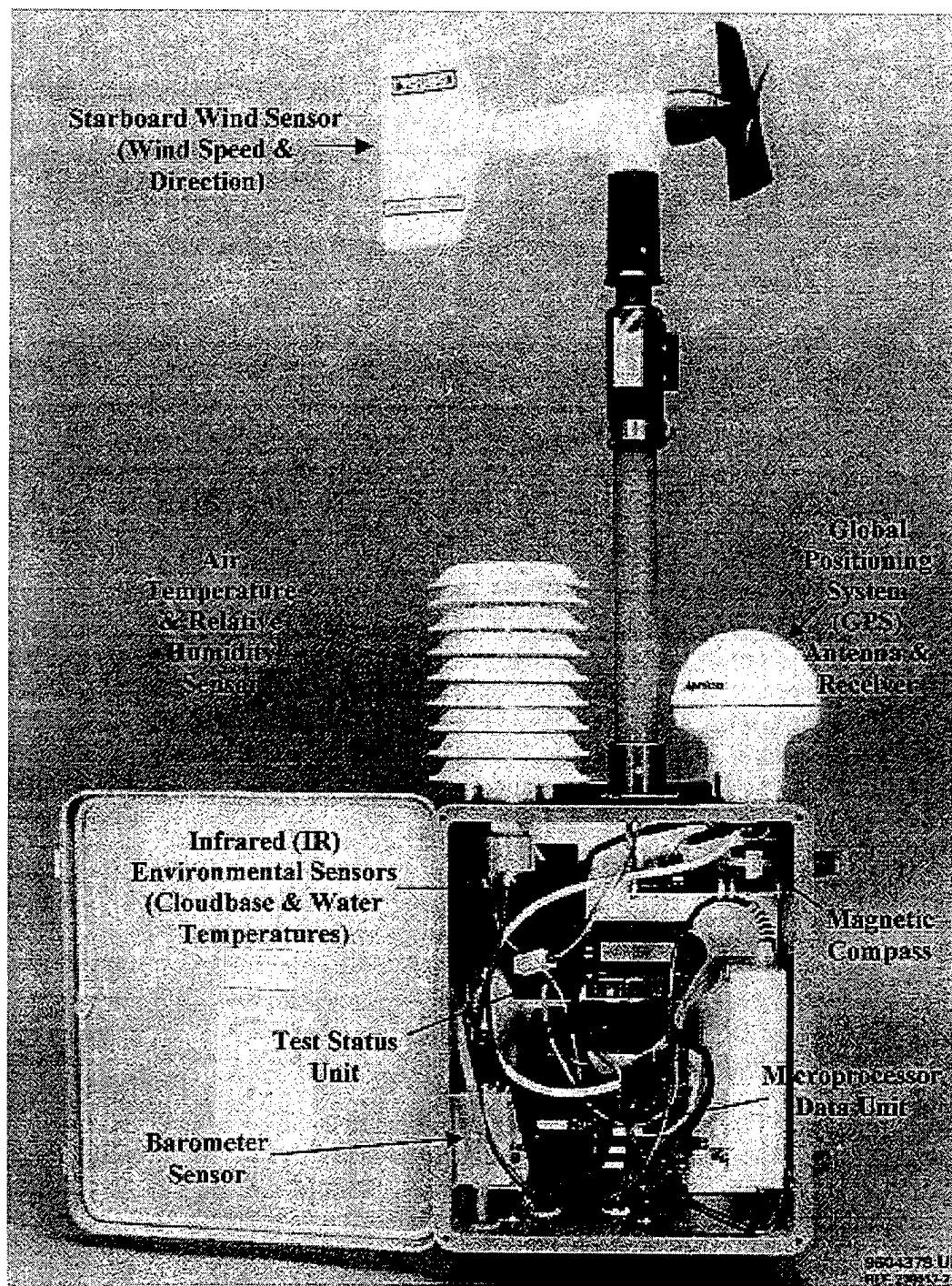
Figure 2.2 Port Met Mast components.

Figure 2.3 Starboard Met Mast components.

13

III. ATMOSPHERIC PROPAGATION

A. INDEX OF REFRACTION

Refraction describes the ability of a medium to bend the ray of an electromagnetic wave as it passes through the medium. The degree of bending is determined by gradients of the index of refraction, n, which is related to the ratio of the velocity of propagation in free space, c, to the velocity in the medium (v),

$$n = \frac{c}{v}. \tag{1}$$

Key concepts concerning refraction are reviewed following discussion by Patterson (1988).

Propagation in free space can be related to propagation away from the influence of the earth or other objects. Reduction in field strength, or propagation loss, for free space is defined by the squared inverse of the distance. In free space, the rays traced by EM waves travel in straight lines and radars are basically line of sight. This is not true for EM waves traveling in the atmosphere.

Even with the assumption of a "normal" atmosphere, radars would still have slightly extended over the horizon detection ranges due to the fact that the index of refraction (n) generally decreases with height. EM waves "bend" toward higher values of (n). Rays traveling through the atmosphere are bent toward the surface instead of traveling straight out into space, thus allowing the potential for over the horizon detections.

B.   REFRACTION IN THE TROPOSPHERE

The troposphere is considered the primary medium through which surface based radar EM energy propagates. The normal value of (n) for the atmosphere near the earth's surface varies between 1.000250 and 1.000400 (Patterson, 1988). For studies of propagation, the index of refraction is not a very convenient number because the value is very close to 1. A scaled index of refraction,(N), called refractivity, has been defined based on the difference of n from 1;

$$N = (n-1) \times 10^6. \tag{2}$$

The relationship for the refractivity (N) for any altitude with atmospheric pressure, (P), temperature, (T), and partial pressure of water vapor, (e), is given by:

$$N = (77.6)\frac{P}{T} + (5.6)\frac{e}{T} + (3.73 \times 10^5)\frac{e}{T^2}. \tag{3}$$

Both P and e are in millibars (mb), and T is in degrees Kelvin (K). The near-surface, well mixed atmosphere reveals a temperature decrease with height of 10°C per km (dry adiabatic lapse rate). The entire troposphere is characterized by a temperature decrease with height with the average vertical temperature gradient of 6-7°C per km. The only refractive significant gas that varies with height is water vapor. The water vapor content of the troposphere rapidly decreases with height. Typically at an altitude of 1.5 km the water vapor content is approximately half that of the surface.

Snell's Law predicts the path of an EM ray as it propagates through the medium with varying indices of refraction. It determines the new direction of ray travel as it transitions into a different layer of the medium provided the initial direction of the ray is known. Snell's Law can be used to show that the radius of the ray is determined by the gradient of (n) using the relationship:

$$r = \frac{10^6}{-(\frac{dN}{dz})}.$$
(4)

Since the propagating EM energy will be bent downward from a straight line as the index of refraction decreases with increasing altitude, a more useful and convenient way of describing the atmosphere's refractive condition is in terms of waves traveling in straight lines. This is accomplished by replacing the actual earth's radius with one approximately four-thirds as great which is typically referred to as the effective earth's radius and by replacing the actual atmosphere by one that is horizontally homogenous. The resultant refractivity is called modified refractivity (M). The modified refractivity index can be calculated from the following expression:

$$M = N + 10^6 \frac{z}{R_e}.$$
(5)

where (z) is the height above the earth in km, (N) is the refractivity at that height and (Re)

is the radius of the earth in km. The modified refractivity index typically increases with height in the standard atmosphere. The use of the modified refractivity index is more advantageous to graphically display and identify trapping layers and ducts. Utilization of the refractivity units requires the user to identify where gradients of dN/dz are less than or equal to -157N/km. This can often be difficult to identify when (N) is plotted against height. Also, -157N/km is the vertical gradient that produces ray curvature equal to the earth's curvature. The use of modified refractivity simply requires the identification of negative dM/dz regions to identify the location of trapping or ducting conditions (Hitney, 1995).

C.   ATMOSPHERIC DUCTS

1.   General

The most significant refractive effect on air defense systems involves atmospheric ducting. Ducting occurs whenever a refractivity profile contains at least one trapping layer, where ray curvature exceeds the earth's curvature. This leads to the formation of a radar duct resulting in focusing of radar energy and in propagation ranges beyond free-space or the horizon. There are three types of ducting relevant to ship-based systems: elevated ducts, surface ducts, and the evaporation ducts. It is the evaporation duct that will be the focus of this thesis.

2.   Evaporation Duct

The evaporation duct is found over all oceanic surfaces and is caused by strong humidity gradients immediately above the air-sea boundary. The rapid decrease in relative humidity creates a trapping layer adjacent to the surface which becomes the reflecting base of the resulting duct. In addition to the water vapor content (e) affecting the humidity

18

gradient, the air-sea temperature difference (ΔT), and wind speed (U) also impact trapping layer duct formation and height through their role in mixing. Increased mixing will decrease gradients except immediately above the interface.

As presented, modified refractivity (M) is a function of pressure, temperature and humidity and dM/dZ=0 corresponds to evaporative duct height (Fig. 3.1). Z_*, the duct height can be expressed as the level where,

$$dM/dZ = 0 = .3dp/dZ + 7.2dq/dZ - 1.4dT/dZ + .157m^{-1} \qquad (6)$$

where q=.622e/p. This illustrates that Z_* is determined by the pressure, temperature, and humidity gradients. Wind speed (U) is a factor on duct height formation since it affects the stability of an area. Stability functions, $\phi(\xi)$, have been determined empirically (Fairall et. al. ,1996) for use in determination of Z_*. The following expressions relate the gradient from above to surface layer scaling parameters and the stability functions:

$$dq/dZ = [q_*/\alpha kZ]\ \phi_s(\xi) \qquad (7)$$

$$dT/dZ = [T_*/\alpha kZ]\ \phi_s(\xi) \qquad (8)$$

$$dU/dZ = [U_*/kZ]\ \phi_s(\xi) \qquad (9)$$

where (α) is the diffusivity constant (1.35), (k) is the von Karman's constant (.35), and $\xi = Z/L$, with (L) being the Monin-Obukhov stability length (Monin and Obukhov, 1954),

$$L = Tu_*^2/[kg(T_* + .18q_*)].$$ (10)

Combining the previous equations gives an expression for Z_* (Fairall, et. al., 1996);

$$Z_* = -\frac{[7.2q_* - 1.4T_*]}{.121\alpha k}\phi_s(\xi_*)$$ (11)

where $\quad \xi_* = Z_*/L.$

Tactically, the duct height is important because it provides a measure of the strength of the duct. Normally Z_* is in 0-40m. Typically, the lowest frequency affected by the duct is generally around 3GHz. Evaporation ducts allow for extended ranges of surface to surface radio or radar systems operating above 3GHz. They also tend to be "leaky" and may affect radar terminals above as well as within the duct(Hitney, 1995). The equation for determining frequency is significantly affected as a function of duct height is:

$$f_m = (3.60 \times 10^{11} Hz/m^{-3/2})Z_*^{-3/2}.$$ (12)

Frequency higher than (f) is significantly affected. These frequencies become lower as duct height increases.

Figures 3.2&3.3 illustrate the sensitivity of duct height on wind and humidity on duct height. In particular, Figure 3.2 illustrates the duct height increases if the air-sea temperature difference is positive or stable conditions exist and mixing is reduced resulting

in a steeper humidity gradient above the surface. Additionally, lower wind speeds mean less mixing of the water vapor, thus the gradient remains larger and higher duct heights result. The more stable the environment near the sea surface the greater the duct height and conversely the more unstable, the lower the duct height. It is important to note that for stable conditions and light winds, accuracies of +/-.5°C are important for estimating the evaporative duct. The influence of wind on Z_* is the reason for examining satellite sensed winds in this study.
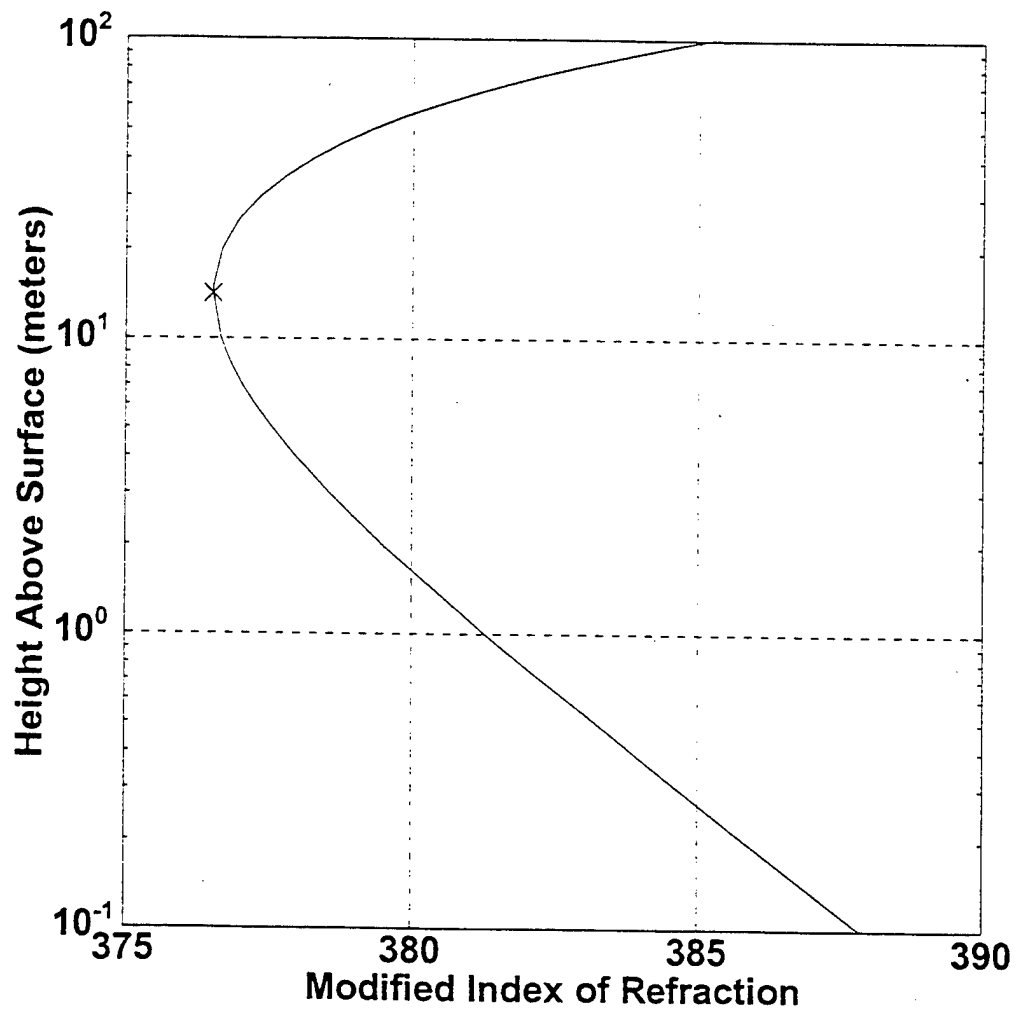
Figure 3.1 Example of M-Profile. Top of evaporative duct is indicated by the "x".

Figure 3.2 Impact of Wind Speed on Evaporative Height.

23

IMPACT OF HUMIDITY ON EVAPORATION DUCT

EVAPORATION DUCT HEIGHT (feet)

WIND SPEED = 7 knots

$T_{air} - T_{sea} = +0.5\ ^\circ C$

$T_{air} - T_{sea} = -0.5\ ^\circ C$

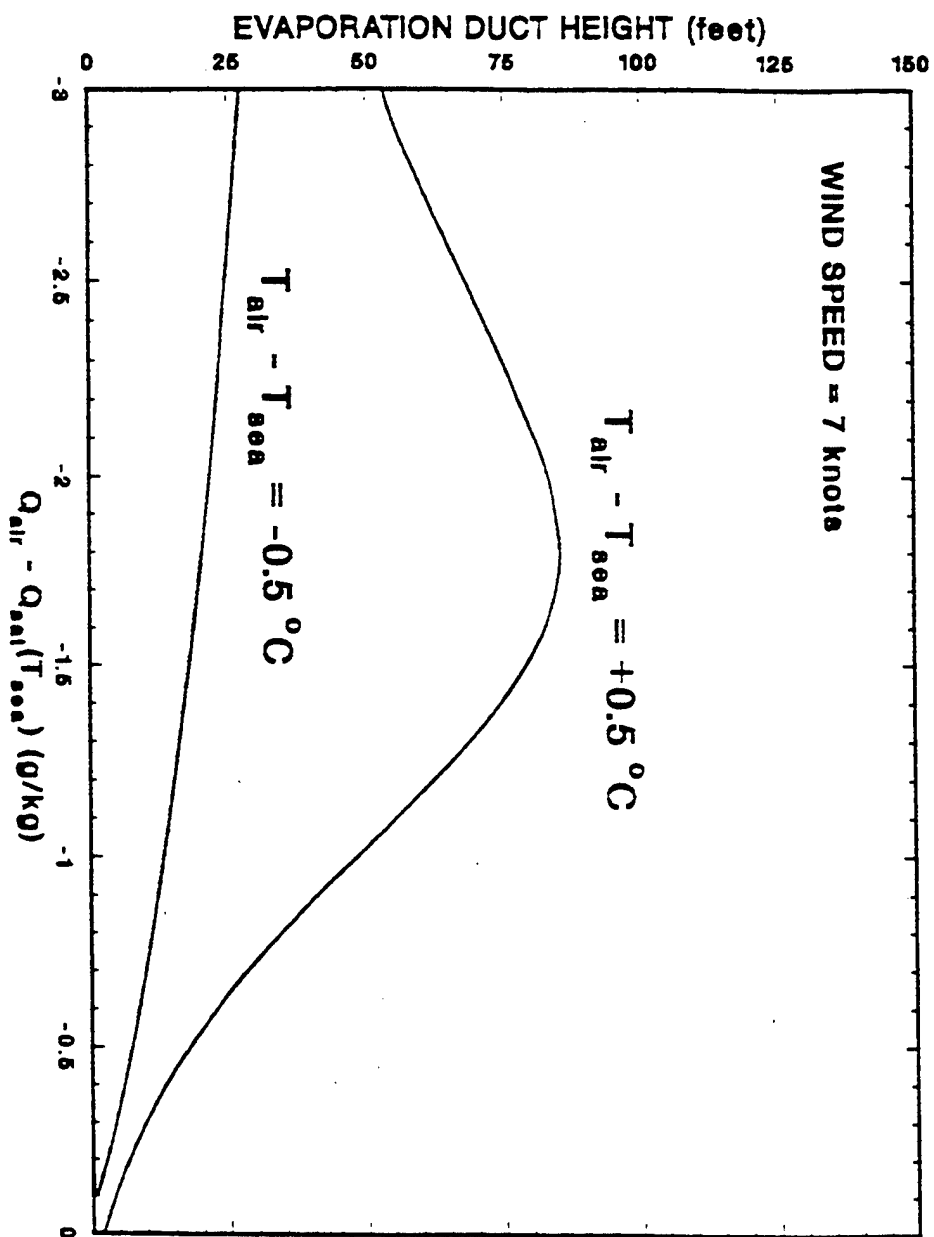$Q_{air} - Q_{sat}(T_{sea})\ (g/kg)$

Figure 3.3 Impact of Humidity on Evaporative Duct Height.

24

IV. PROCEDURE

A.   OVERVIEW

1.   Bulk Method

The most common occurring anomalous propagation phenomenon over the ocean is the evaporative duct. Given its significant impact on the propagation of radar and the relationship of duct height to frequency affected, it is important to understand the models or methods currently in use today for calculating the duct height. Since the refractive profile is a function of pressure (P), air temperature (T), and humidity (q), its estimation with respect to height (Z) will be difficult because of the non-availability of multi-level measurements. However, a method called the Bulk Method, can be used based on measurements at a single level and knowledge of the surface layer structure.

This basic approach for all evaporation duct models involves expressions for the vertical refractivity gradient in terms of atmospheric variables using the bulk measurements as described in the last chapter [equation(6)]. This expression is then solved for duct height given the dM/dZ=0 at the top of the duct. Since the duct is limited to the surface layer, a similarity theory such as Monin and Obukhov (1954) is useful for deriving the expression (Babin, et. al., 1997). To do this requires an integral form of the equations (7-9) in order to relate q_*, T_*, and L in equation (11) to bulk parameters (Fairall, et. al., 1978). The resulting equation is:

$$Z_\star = -\frac{[7.2\Delta q - 1.2\Delta T]}{.125[Ln\ Z/Z_o - c(u)]}\phi_s(U) \qquad (13)$$

This equation allows $Z_\star$ to be obtained from bulk measurements; surface temperature, air temperature, humidity, and wind speed.

2.   M-Profile Method

The M-Profile Method for determining the evaporative duct properties such as height is used in this thesis to run RPO to obtain a propagation loss information. This is because input to RPO is M values at multiple levels. Since this paper was only concerned with the surface layer, the method permitted the use of small increments in describing the profile of the lower 100m. The M-profile method requires obtaining scaling parameters; $U_\star$, $T_\star$, $q_\star$, and L from the measured data and a parameterization model (Fairall, et. al., 1978). These parameters are then used in combination with empirically derived (ϕ) functions to obtain profiles of temperature and humidity. The pressure profile is obtained assuming hydrostatic conditions. With separate profiles of atmospheric parameters, values are taken to compute M at levels using the M-profile equation:

$$M(Z) = (77.6)\frac{p(Z)}{T(Z)} - (5.6)\frac{e}{T(Z)} + \frac{(3.73)\times10^5 e}{T^2(Z)} + 0.1 \qquad (14)$$

This creates an M-profile used for RPO input. The evaporative duct height is specified at

26

the location where dM/dZ=0.

B. REFRACTIVITY MODELS

1. Radio Physical Optics (RPO)

RPO was developed by the Naval Command, Control and Ocean Surveillance Center RDT&E Division (NRAD) for the purpose of calculating EM system propagation loss within a heterogeneous atmospheric medium where the index of refraction is allowed to vary horizontally. The current version, 1.15, was incorporated in the Oceanographic and Atmospheric Master Library (OAML) in January 1996.

RPO determines field strength versus height and range for surface transmitters and paths that are over water only. It is a hybrid model combining the use of Ray Optics (RO) and Parabolic Equations (PE) approaches, to account for range-dependent vertical refractivity profiles. It incorporates geometric optics and extended optics in other areas to enhance coverage over a large range and altitude regions. Figure (4.1) illustrates how RPO utilizes this hybrid approach that uses the complimentary strengths of both RO and PE methods to construct a fast and highly accurate composite model. This has resulted in RPO running at 25 to 100 times faster than the PE model alone, while still achieving accuracy near that of pure PE models.

RPO is restricted to frequencies from 100MHz to 20GHz and is applicable for antenna heights from 1 to 100m. Features include the ability to select: horizontal, vertical, or circular polarization; omni, Gaussian, sin(x)/x, cosecant-squared, generic height finder, or user defined height finder antenna pattern; vertical beamwidth from 0.5 to 45 degrees;

27

antenna elevation angle from -10 to 10 degrees; presence or absence of tropospheric scatter and gaseous absorption. For this thesis a frequency of 3.3GHz, vertical polarization, sin(x)/x antenna pattern, and zero elevation angle were used in comparing the propagation loss curves.

2.   Engineer's Refractive Effects Prediction System (EREPS)

A derivative of the Integrated Refractive Effects Prediction System (IREPS), EREPS was designed for engineers to allow for greater flexibility to edit parameters and display effects in assessing atmospheric refraction. The EREPS program, PROPR, creates the propagation-loss-versus-range plots from RPO predictions.

PROPR uses the output file from RPO and plots the propagation loss curve as a horizontal slice of that coverage diagram. PROPR calculates and displays propagation loss in a decibel versus range graphic. Propagation mechanisms considered in the program include; optical interference, diffraction, tropospheric scatter, evaporation ducting, surface-based ducting, and water vapor absorption. (Patterson, et. al., 1994)
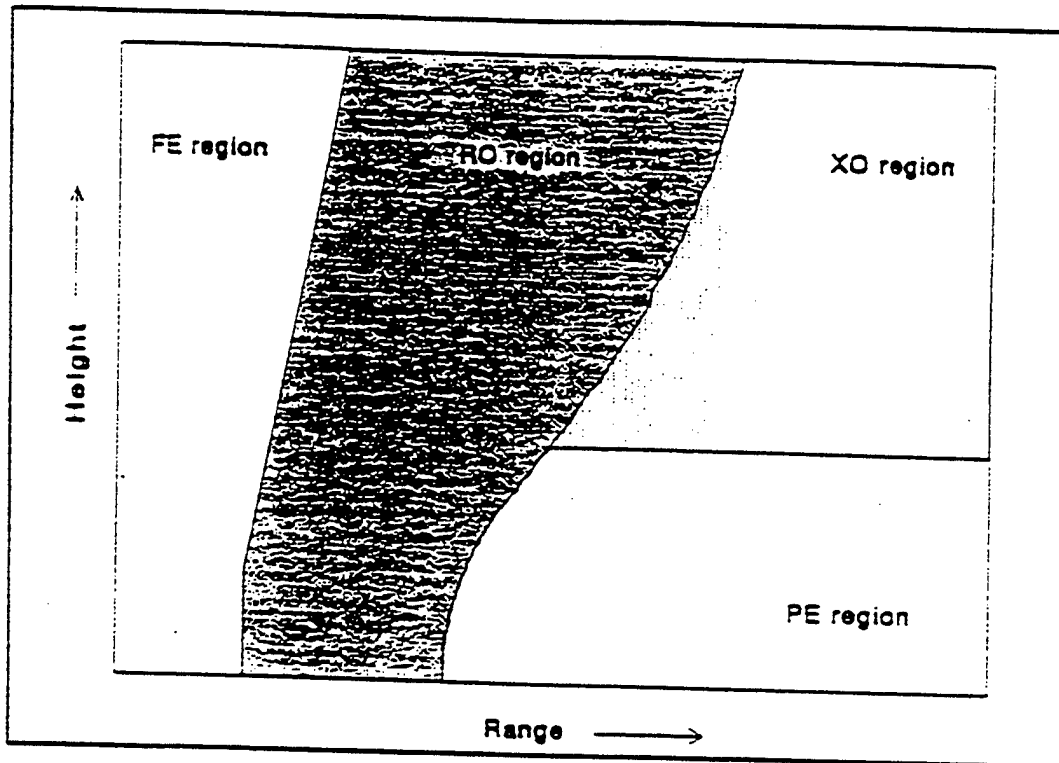
Figure 4.1 RPO calculation regions (after Patterson and Hitney 1992).

V. EVALUATION OF MEASUREMENT SYSTEM

A.   DATA SELECTION

Atmospheric and ocean surface data used in evaluation of the measurement systems and evaporation duct descriptions were collected during an annual summer exercise, BALTOPS '97, by the USS ANZIO (CG-68) and USS CAPE ST GEORGE (CG-71). Both ships left Norfolk, VA in late May 1997 for a North Atlantic transit, arriving in the Baltic Sea in early June, with several stops en route. Both ships, outfitted with the SEAWASP sensor, remained together for the majority of the two month period except for a few different port calls within the Baltic Sea region. Due to the ships being in proximity of each other and also to inconsistencies on when SEAWASP was activated, both ships were treated as one for data analyses purposes. For final analyses, data corresponding to the June period were collected onboard CG-71 and data corresponding to the July period were collected onboard CG-68.

Several factors were considered in selecting a sample set for analyses. These included: underway time during each day since the ships spent considerable time in port due to the nature of the exercise, geographic location, and whether a satellite pass from the ERS-2 scatterometer had a footprint near the ship's position. Of interest was whether a pass was usable for evaluating the remotely sensed winds.

The result of the selection based on these factors was that 24 days initially met the underway time requirement. The number of days finally considered were reduced to six which were used in comparisons of the evaporative ducts estimates. These comparisons

were based on the factors mentioned above, as well as on how the periods illustrated variability of parameters influencing the duct. Of these six days, three have satellite information. The eighteen days not discussed showed similar results as the chosen six and therefore are not presented in this thesis.

Some adjustments were necessary to more accurately reflect how the different measurement systems and procedures affected the calculated duct height. First, the SEAWASP system used an IR sensor directed at a 45 degree depression angle towards the surface and covered by a thin transparent window to measure the sea surface temperature (SST). Unfortunately, the sensor gave consistently high sea surface temperatures. The reason for this error in the IR sensor derived SST was that the optical window over the sensor was contaminated by sea salt. Therefore, the IR thermal image view was not of the sea surface but rather of the salt on the window which, when warmed by the sun, yielded the inaccurate IR SST readings. Consequently, the only remaining choice for the sea surface temperature was that measured by a thermostat located at the ship's intake under the keel. Due to the draft of the ship, it is not an accurate measure of temperature at the sea surface. The intake temperature value, as well as the other parameters needed for duct height calculation, were recorded in the bridge navigation logs . Copies of the logs were obtained from the USN climatological detachment in Asheville, NC.

. There was different measurement frequency between the bridge log and SEAWASP. This is because SEAWASP measured data continuously and saved five minute averages, but the bridge observations were only taken at exactly five minutes to the hour, every hour. Evaporation duct heights in the SEAWASP time series plots were calculated

with SST interpolated between the hourly bridge observations to five minute intervals to replicate SEAWASP sampling frequency.

A second adjustment to measured and recorded values was necessary because the ship's and SEAWASP sensors were at different levels. The SEAWASP sensors were at approximately 29ft above the surface, while the ships temperature and humidity senors were made at the bridge height of 60ft and the wind senors were at a main mast yardarm height of 75ft. The height differences of multi-variable measurements were accounted for in the calculations by adjusting values to different heights as predicted by surface layer scaling with proper accounting for effect of thermal stratification. In neutral conditions the adjustment is based on logarithmic change with height.

A goal in this study was to evaluate the operational use of satellite derived winds for estimating evaporation duct conditions. This is important because the wind speed is a critical parameter in the evaporation duct calculation. Furthermore, satellite derived winds provide the spatial variation of this parameter and spatial variations are important when predicting of extended radar ranges. Unfortunately, the joint availibility of scatterometer and SEAWASP winds within this two month period was not achieved. It was hard to obtain a "hit" with the ERS-2 scatterometer due to the orbit pattern of the satellite and the ships track. This was especially true in the Baltic region where the scatterometer data was sparse due to the proximity of the surrounding landmass. In addition, a second scatterometer on the Japan ADEOS satellite failed early in the data period.

There were three days when the satellite footprint and the ship's locations were close. For these three days the scatterometer winds as well as the SEAWASP winds were merged

with the remaining SEAWASP measurements to calculate a "satellite duct height".

B.   RESULTS: DEMONSTRATING MEASUREMENT SYSTEM DIFFERENCES

1.   General

Six days are used to illustrate the differences between SEAWASP and existing ship

measurements for estimating evaporation duct properties. The days represent data from the

Denmark Straits and Baltic Sea to the North Atlantic and Mid-Atlantic East Coast region.

The days are distributed over the June/July time period with the last three days focusing on

the end of the cruise, as the ships returned to their homeport of Norfolk.

The days were also selected in order to illustrate differences in particular parameters

used to calculate duct height. Days with high and low humidities and wind speeds were

compared as well as days with differing stability conditions based on air-sea temperature

differences. In the following discussion the following points will be addressed: the effect

of differences in measured quantities of the evaporation duct, reaction time differences due

to evaporative duct changes, the implications for operational roles of satellite winds for

evaporation duct assessment, and the impact of continuous versus one-hour data acquisition.

Table 5.1 provides values of the selected days which will be used in the discussion.

As stated, evaporation duct information was based on a method that only gave duct

height, (Babin et. al., 1997), and also on determining the M-profile. The duct height values

from Babin's approach were used for the time series figures in the following discussions.

M-profiles were used to obtain values for RPO.

34

TABLE 5.1

Sensor	Date	U (m/s)	Ta ©	Ts ©	RH(%)	P (mb)	Z* (m)	La/Lo
6/11/97	Bridge	4.2	12.8	11.1	83	1014.1	**58.3**	54.4/007.1
(0255Z)	*Seawasp*	6.6	13.7	11.1	86	1018.7	**0.8**	54.4/007.1
6/25/97	Bridge	9.3	12.8	12.2	86	1002.6	**4.0**	55.5/016.3
	Seawasp	9.5	12.7	12.2	82	1007.6	**5.8**	55.5/016.3
(1955Z)	**Satellite***	**9.0***	12.7	12.2	82	1007.6	**6.0**	55.5/016.3
7/08/97	Bridge	10.3	18.3	15.6	65	1011.4	**24.5**	58.7/020.1
(2155Z)	*Seawasp*	7.3	15.7	15.6	77	1015.8	**9.8**	58.7/020.1
7/26/97	Bridge	13.9	20.0	21.1	70	1013.1	**14.8**	40.8/048.3
	Seawasp	13.2	20.1	21.1	93	1016.9	**5.2**	40.8/048.3
(1555Z)	**Satellite***	**7.0***	20.1	21.1	93	1016.9	**5.4**	40.8/048.3
7/28/97	Bridge	9.3	26.1	27.8	79	1010.0	**14.3**	38.8/062.2
(0655Z)	*Seawasp*	0.9	24.6	27.8	92	1013.2	**3.8**	38.8/062.2
7/29/97	Bridge	9.8	26.7	26.7	91	1005.6	**6.1**	37.5/071.1
	Seawasp	1.9	26.2	26.7	99	1009.0	**1.2**	37.5/071.1
(0555Z)	**Satellite***	**6.0***	26.2	26.7	99	1009.0	**1.4**	37.5/071.1

2.   Wind Speed Effects and Duct Height Variability on 11 June 97

Data collected by the SEAWASP system and by bridge personnel are shown (Fig.

5.1). The time series indicate the data frequency and variability of the measured parameters

used to calculate the evaporation duct height. The parameters are wind speed and direction,

relative humidity, and air and sea temperature. The top graph depicts the calculated duct

35

height based on values contained in the lower three graphs. Figure 5.1 depicts air and sea temperatures in the lower graph and the interpolation of sea temperature for SEAWASP data points is clearly observed. In this particular case, conditions are stable based on the temperatures measured for this day. Other time series graphs depict the relative humidity trends, wind speed and direction trends.

On this day the ship was located 65nm south-southwest of Esbjerg, Denmark, approaching the Skagerrak. Differences among the time series show a 2-4°C air temperature difference between air temperatures from 13Z-18Z on this day. Likewise, there was a wind speed difference during the afternoon with SEAWASP winds tapering off to light wind while bridge observations maintains the winds at 9-10 m/s. In this case, continuous measurement was crucial in describing the rapidly changing duct height due largely to a significant change in wind speed and direction at mid-day. During this day, already under stable conditions, there was a wind shift coupled with a rapid decrease in speed which resulted in large duct heights. Had scatterometer winds been available for this time period, a tactical coordinator could have been able to predict, with reasonable certainty, changes in duct height which equates to changes in radar propagation predictions. Additionally, the ship's relative humidity from the early morning hours to the mid-afternoon, depicts unusual variability compared to the relatively constant mean of 80% measured by SEAWASP. This example clearly illustrates differences in the evaporative duct heights due to different observation methods.

The variability in duct height impacts decisions on a tactical level by looking at measured values at 0255Z on 11 June 1997 (Table 5.1). Note the significant difference in

evaporation duct heights for the ship and SEAWASP respectively. Refering to Table 5.1 and Figure 3.2, this illustrates the impact, under highly stable conditions, how a slight difference in air-sea temperatures and in wind speeds can dramatically influence duct heights. This directly translates into tactical terms when the duct heights are used to compute a propagation loss diagram (Fig. 5.2). Here, the propagation loss diagram, which depicts radar energy lost (db) over range, indicates that if the SPY-1 radar used the SEAWASP data instead of ships obtained data, a 10 nm loss in radar range occurs. Assuming the inbound target to be traveling near mach, this equates to approximately a one minute reduction in reaction time for ship defense systems to counter the threat.

Furthermore, this variability is shown (Fig. 5.3) during a one hour time period. The ship recorded a duct height of zero from 0855-0955Z while the SEAWASP system estimated duct heights from 5.2m to 4.6m then up to 7.1m and then to 4.0m. This equated to detection ranges varying from 16nm to 13.5nm based on SEAWASP measurements. Without the advantage of continuous measurements, none of this variation would have been detected and therefore compensated for by the radar controller.

3. Satellite Wind Comparison on 25 June 97

This day was chosen for analyses because of the availability of wind data from the ERS-2 satellite. The ship was operating in the Baltic 75nm northwest of Gdansk, Poland. The time series (Fig. 5.4) for the period shows good agreement between SEAWASP and bridge measurements for air temperature and wind speed but not for relative humidity. This leads to significant differences in duct height calculated from the two measurement systems. A vivid indicator of the difference between the two systems is the 100% humidity values

37

measured by the ship during the afternoon period when SEAWASP measured values in the 70-80% range. These humidity measurements led to duct heights of 7-10m for SEAWASP while the ship measurements directly correspond to zero duct heights, since there is no vetical moisture gradient.

Further analyses of the data is completed for 1955Z. This time closely corresponds with the satellite pass at 21Z (Fig. 5.5). A comparison of measured and calculated values for this time (Table 5.1) indicates that they are in reasonable agreement. This agreement also applies to the satellite derived wind speed obtained from the ERS-2 scatterometer. Figure 5.5 illustrates the spatial variation of satellite interpreted winds as well as the gaps in coverage that are present in the satellite swath. This depiction will be repeated in follow-on satellite figures later in this chapter.

The tactical impact for this data time (Fig. 5.6) is only a 6 sec increase in detection time. There was minimal propagation loss versus range and therefore little difference in reaction time due to evaporative duct differences. However, had a pair of data points from the afternoon period been chosen, there would have been significant differences in propagation loss ranges due to the difference in duct heights.

4.   Evening Variability of Duct Heights on 08 July 97

During this period the ship was operating 120 nm south of Stockholm, Sweden. The period was selected for discussion because of parameter differences throughout the time series plots (Fig. 5.7). Significant variations occurred during the late evening period. During this period the ship's evaporation duct heights became significantly larger than the SEAWASP heights because of measured lower values of relative humidity. The

SEAWASP's winds were less than the ship's winds which would lead to greater duct heights for SEAWASP; however, this reduced mixing condition was not enough to offset the impact of the humidity gradient on duct height. Over the course of the day calculated duct heights increased from 2m to 20m for data from both measurement systems. This illustrates the need for constant attention to changing duct height parameters for radar propagation ranges.

A comparison of one of these evening data points indicates considerable differences in the air temperature and humidity measurements (Table 5.1). Duct heights of 24.5m and 9.8m were calculated using the ship and SEAWASP data respectively. These duct height differences correspond to an approximate 50 sec reduction in reaction time using SEAWASP data versus ship data based on mach 1 missile speed and RPO determined propagation loss versus distance profile (Fig. 5.8).

5.   Satellite Wind Comparison on 26 July 97

This period (Fig. 5.9) occurred when the ship was in transit back to the U. S. East Coast. The location was 540 nm southeast of Newfoundland. This period was selected because the sea temperature was greater than the air temperature. This occurrence is most probably caused by the presence of the Gulf Stream Current. Another reason this case was selected was that the ship was near the footprint of the scatterometer pass at 14Z (Fig. 5.10). Finally, this time series reveals the impact of continuous measurements offered by SEAWASP as well as the accuracy. The variability of the continuous SEAWASP humidity measurements compared to the constant, low bridge observations illustrates this point.

Of note is the lack of SEAWASP data during the latter part of the day. This is due to SEAWASP's internal programming being able to sense erroneous data and therefore not

39

calculating duct heights during that period. This provides further evidence of SEAWASP's ability to provide reliable data through internal quality control of its measured data.

Figure 5.11 is a propagation loss diagram that reflects the difference in duct heights of 14.8m from the ship to 5.2m the SEAWASP measured at 1555Z. From a tactical perspective the propagation loss versus distance profiles yield a 6 nm or 36 sec difference. This results in another example of less reaction time to an incoming threat using the SEAWASP data.

The satellite obtained wind speed was 6.2m/s less than the SEAWASP wind speed but when used in calculating the evaporation duct height, it resulted in only 0.2m difference (Table 5.1). The satellite wind speed difference did not change the propagation loss ranges much because of the impact of other parameters. Under unstable conditions, when water is warmer than air, wind speed dependence of the evaporation duct is not as large (Fig. 3.2). Also, the humidity differences measured in the late morning and then steady rise in the mid-afternoon coupled with slightly unstable atmospheric conditions measured during the day due to the air-sea temperature gradient contributed more to the duct height disparity than the wind measurement differences.

6.   Near-surface Unstable Conditions (Tw>Ta) on 28 July 97

During this period the ship was transiting southeast, 360 nm east-southeast off Boston, MA. This period was selected because of the unstable conditions and to highlight again the value of continuous measurements. SEAWASP (Fig. 5.12) depicts significant variability throughout the time series for relative humidity and wind data compared with the relatively constant measurements obtained by the bridge. Of particular interest on this day

is the consistent presence of unstable conditions due to the air-sea temperature gradient, again due to the Gulf Stream Current. The instability tends to reduce the evaporative duct heights because of the mixing from buoyant forces.

The relationship between measured humidity values and wind speed values appear to compliment each other. The ship recoreds lower humidity values than SEAWASP. This leads to higher duct heights due to the larger gradient (Table 5.1). Also, the ship observed higher wind speeds than SEAWASP which leads to higher duct heights because of the unstable conditions (Fig. 3.2). The result is that both of these factors contribute to the ship duct heights being greater than the SEAWASP heights.

Examining the data at 0655Z, the effect of the differences , tactically, is the ship bridge data predicts extended radar coverage. Actually the ship has approximately 36 sec less reaction time to counter an incoming threat because of the reduced evaporative duct heights derived from data recorded by SEAWASP (Fig. 5.13).

7.   **Satellite Wind Comparison and Duct Height Variability on 29 July 97**

The last period examined had the ship transiting 150 nm northeast of Norfolk, VA just prior to completing its cruise. The period's selection occurs because it includes at satellite pass at 03Z and it clearly shows the relationship of the measured parameters impact on the duct heights, especially from 17Z to 20Z. It also illustrates another example of the value of continuous measurements by the SEAWASP sensor on changing duct heights.

The time series (Fig. 5.14) reveals significant differences in humidity and wind measurements between SEAWASP and the bridge throughout the morning until mid-afternoon. The values are in more agreement during the end of the day. It is this agreement,

somewhat contrary to the other cases, that demonstrates the important relationship of humidity and wind speed on the calculation of evaporative duct heights. Whether it was ship observed data or SEAWASP data, this period's time series shows lower humidity values will raise duct heights and increasing wind speeds in an unstable environment will also increase the duct heights. Had there been stable conditions, higher wind speeds would have had the opposite effect on duct heights. In this particular case, humidity dominates the calculations because the wind speeds, while increasing, remain relatively low.

It was possible to make a partial evaluation of the value of satellite derived wind for this case. Because of intermittent data from SEAWASP, the 03Z satellite pass (Fig. 5.15) was extrapolated and data from 0555Z was used for comparison. Table 5.1 depicts a variety in winds speeds for this time with a 4m/s difference between each of the three observations.

This data were used with RPO and its prediction interpretated using the EREPs propagation loss program. The resulting loss profile (Fig. 5.16) shows only slight differences in the ranges with regard to detection threshold. In this case, 12 sec difference occurred between the ship's expected reaction time and SEAWASP's reduced reaction time. Although 12 sec appears to represent little difference, it is critical in the rapidly changing littoral given future sophisticated high speed missiles.

In illustrating the value of continuous measurements by SEAWASP, the period from 1755-1855Z was examined (Fig. 5.17). During this period, the ship recorded the duct height increasing slightly from 7.6m to 8.2m corresponding to approximately 14 nm detection ranges. However, during the same period, SEAWASP measured and calculated a significant variance in duct heights corresponding to detection ranges of 18.5 nm to14.8 nm that

42

followed an increasing-decreasing-increasing pattern. This flucuating pattern equated to a

total of almost 24 secs of change in reation time for the ship's self-defense forces to counter

an incoming threat at mach speed. Again, as on 11 June, this shows the importance of

continuous measurements of the evaporation duct in adjusting the ship's radar configuration

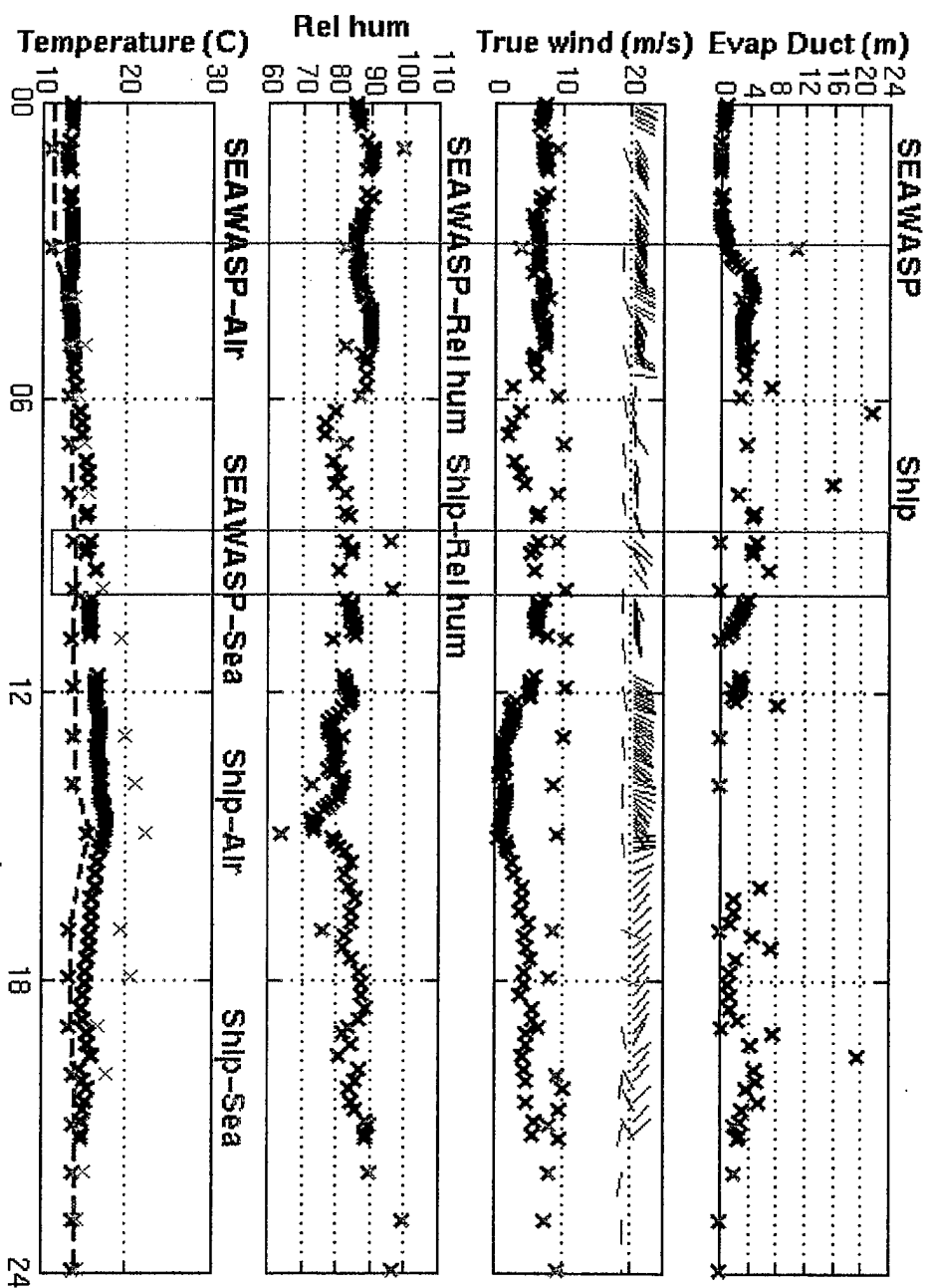for maximum probability of detection.

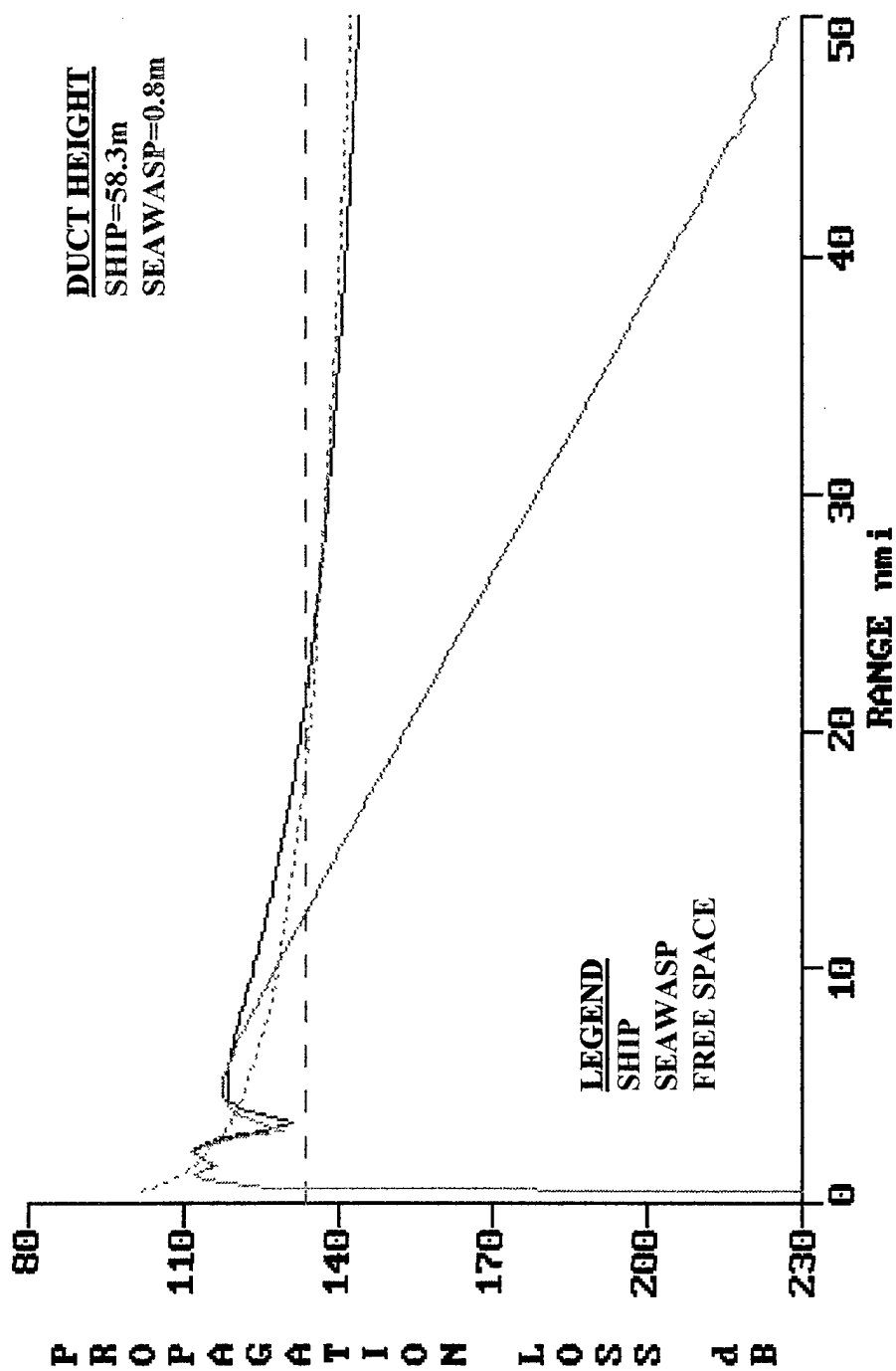**Figure 5.1** Time series for 11 June 1997 (54.5N/007.6E) 65nm SSW of Esbjerg, Denmark.

11 JUNE 1997 (0255Z)

DUCT HEIGHT
SHIP=58.3m
SEAWASP=0.8m

LEGEND
SHIP
SEAWASP
FREE SPACE

PROPAGATION LOSS dB

RANGE nm i

Figure 5.2 Propagation Loss Diagram. Depicts ~10nm difference in detection range.

11 June 1997 (0855-0955Z)

PROPAGATION LOSS dB

DUCT HEIGHT
SHIP (0855Z)=0m
SHIP (0955Z)=0m
SEAWASP(0855Z)=5.2m
SEAWASP(0910Z)=4.6m
SEAWASP(0930Z)=7.1m
SEAWASP(1005Z)=4.0m

RANGE nm i
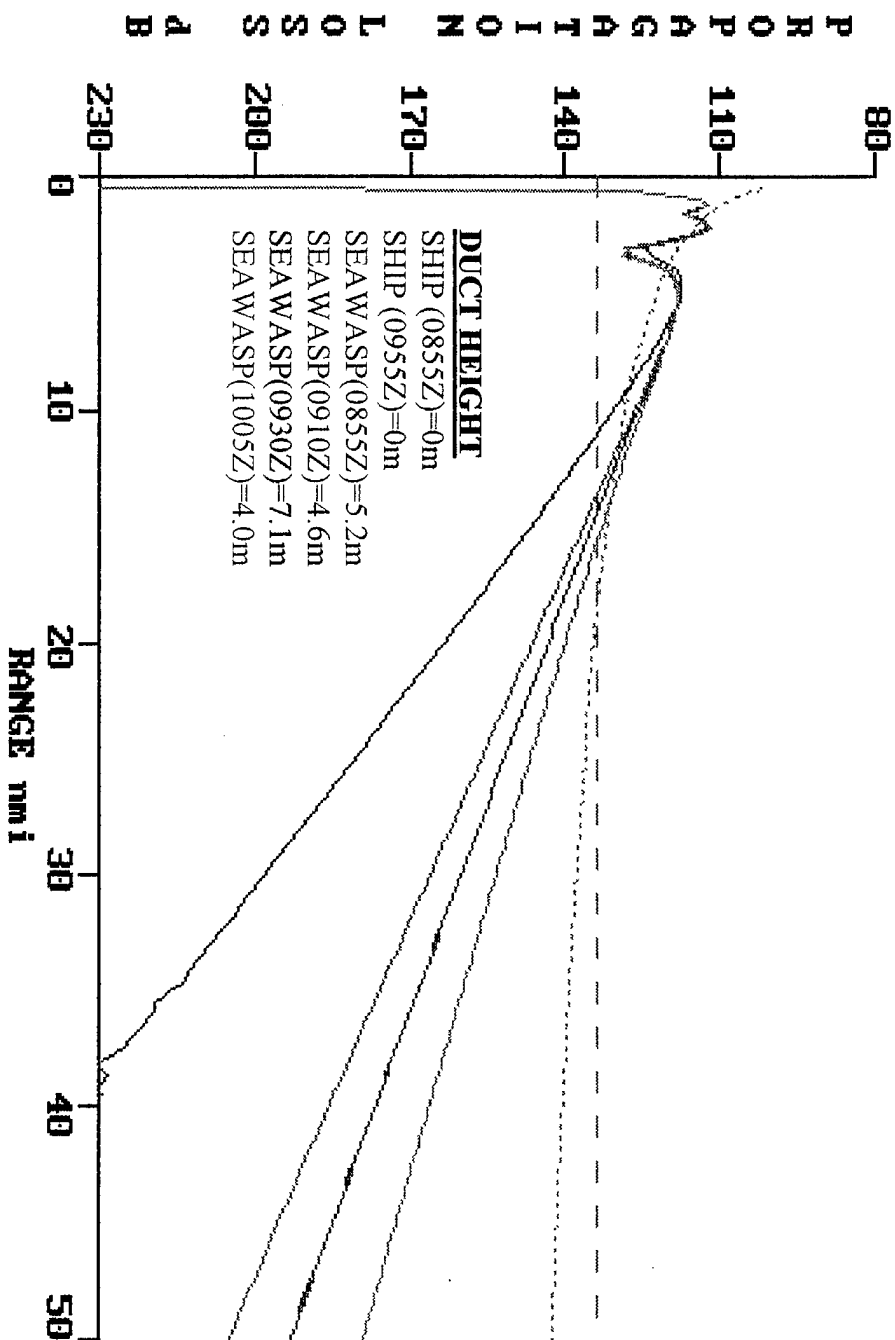
Figure 5.3 Propagation Loss Diagram. Depicts detection ranges due to variability of duct heights during one hour time period.

46
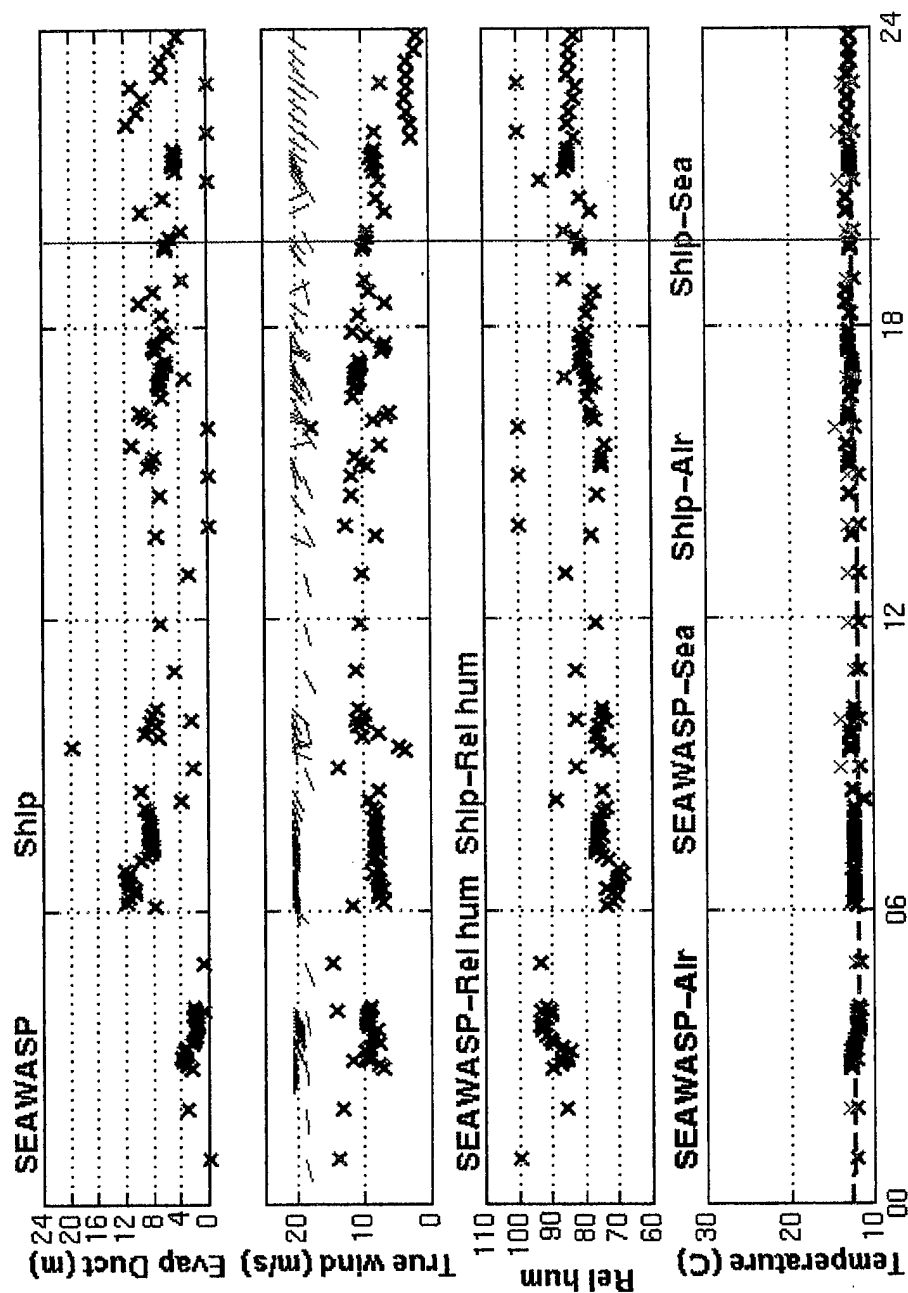
Figure 5.4 Time series for 25 June 1997 (55.4N/018.3E) 75nm NW of Gdansk, Poland.
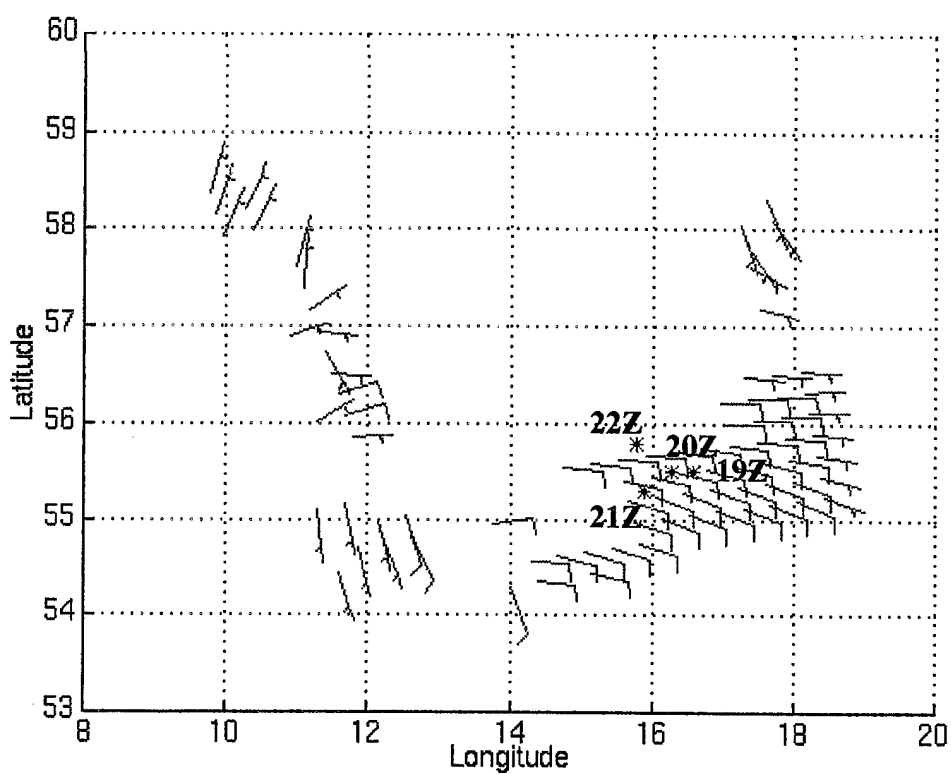
47

Scatterometer Winds for 6/25/97

Figure 5.5 ERS-2 scatterometer winds at 21Z 25 June 1997.

25 JUNE 1997 (1955Z)

DUCT HEIGHT
SHIP=4.0m
SEAWASP=5.8m
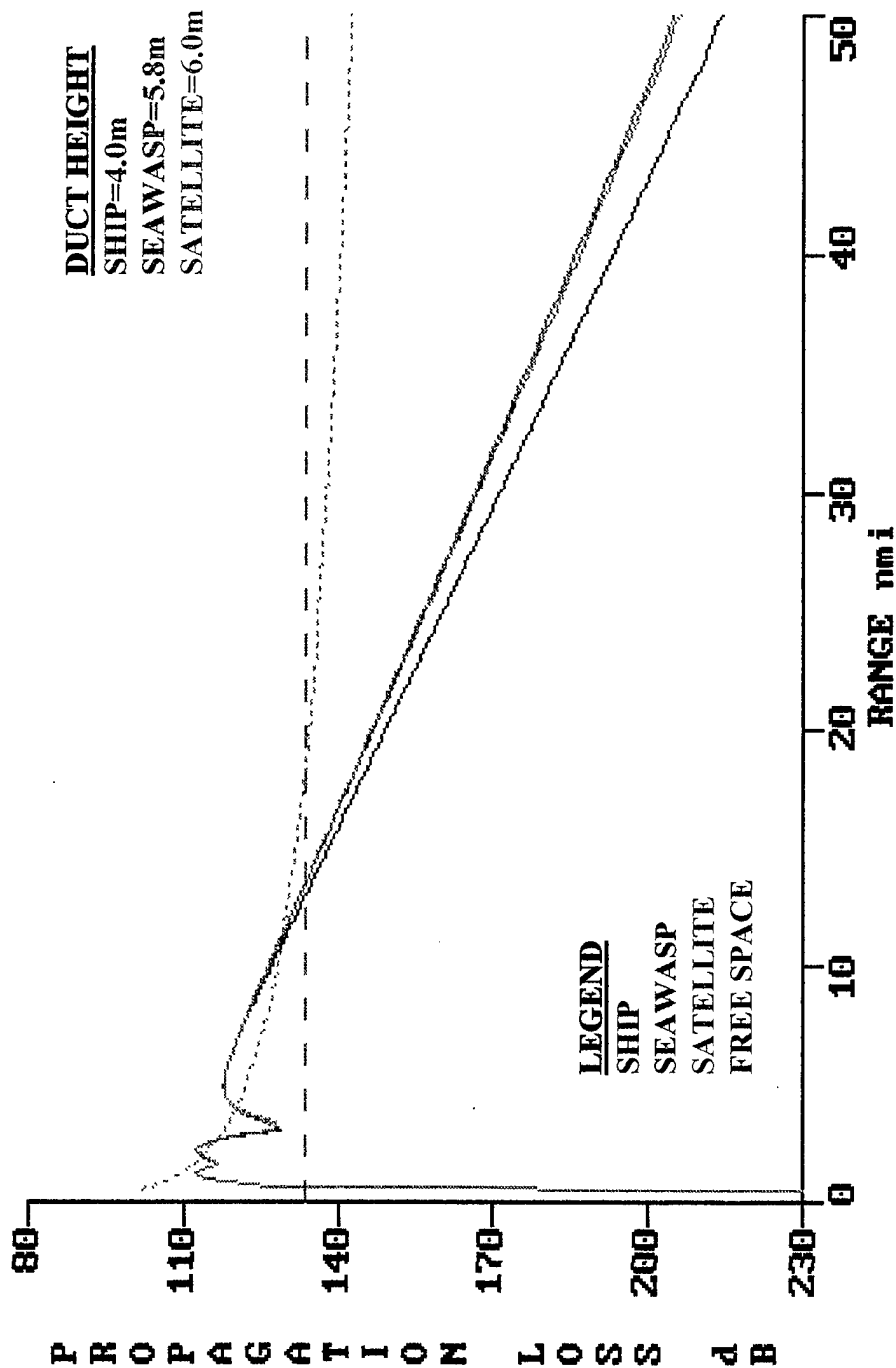SATELLITE=6.0m

LEGEND
SHIP
SEAWASP
SATELLITE
FREE SPACE

Figure 5.6 Propagation Loss Diagram. Depicts ~1nm difference in detection rangebetween SEAWASP and shipboard measurement systems.
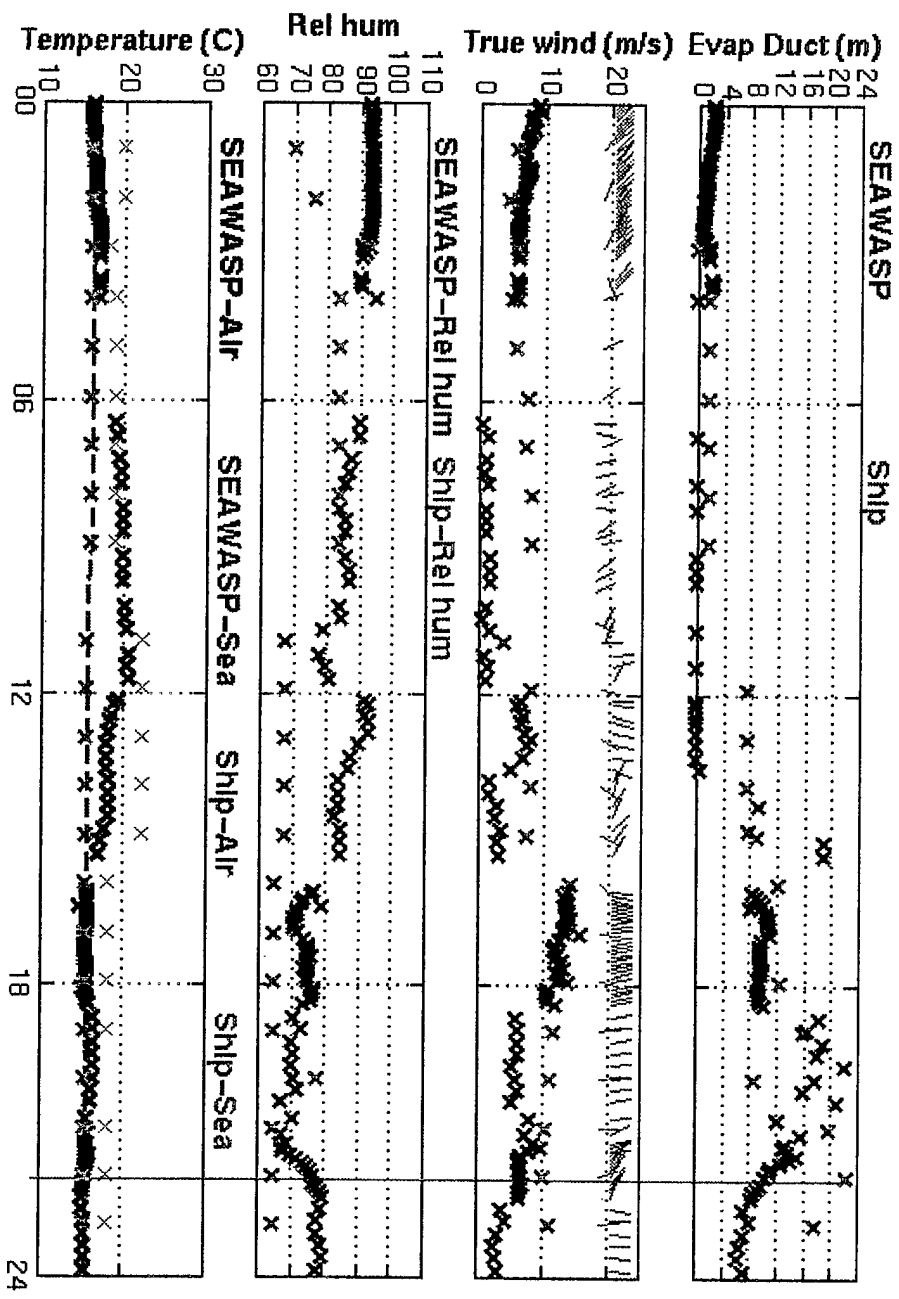
49

Figure 5.7 Time series for 08 July 1997 (57.2N/017.9E) 120nm S of Stockholm, Sweden.

08 JULY 1997 (2155Z)

DUCT HEIGHT
SHIP=24.5m
SEAWASP=9.8m

LEGEND
SHIP
SEAWASP
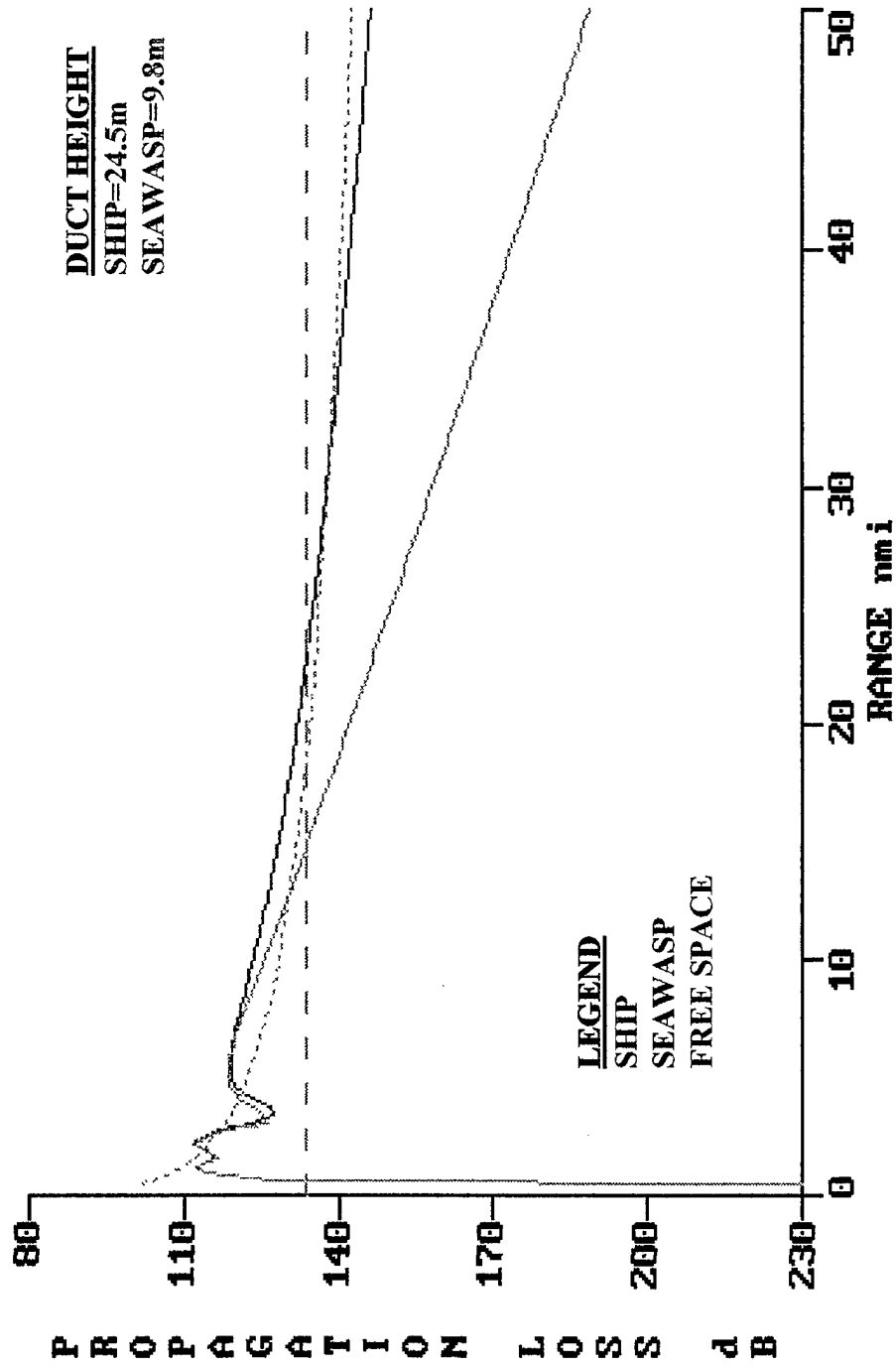FREE SPACE

RANGE nm i

PROPAGATION LOSS dB

Figure 5.8 Propagation Loss Diagram. Depicts ~9nm difference in detection range.
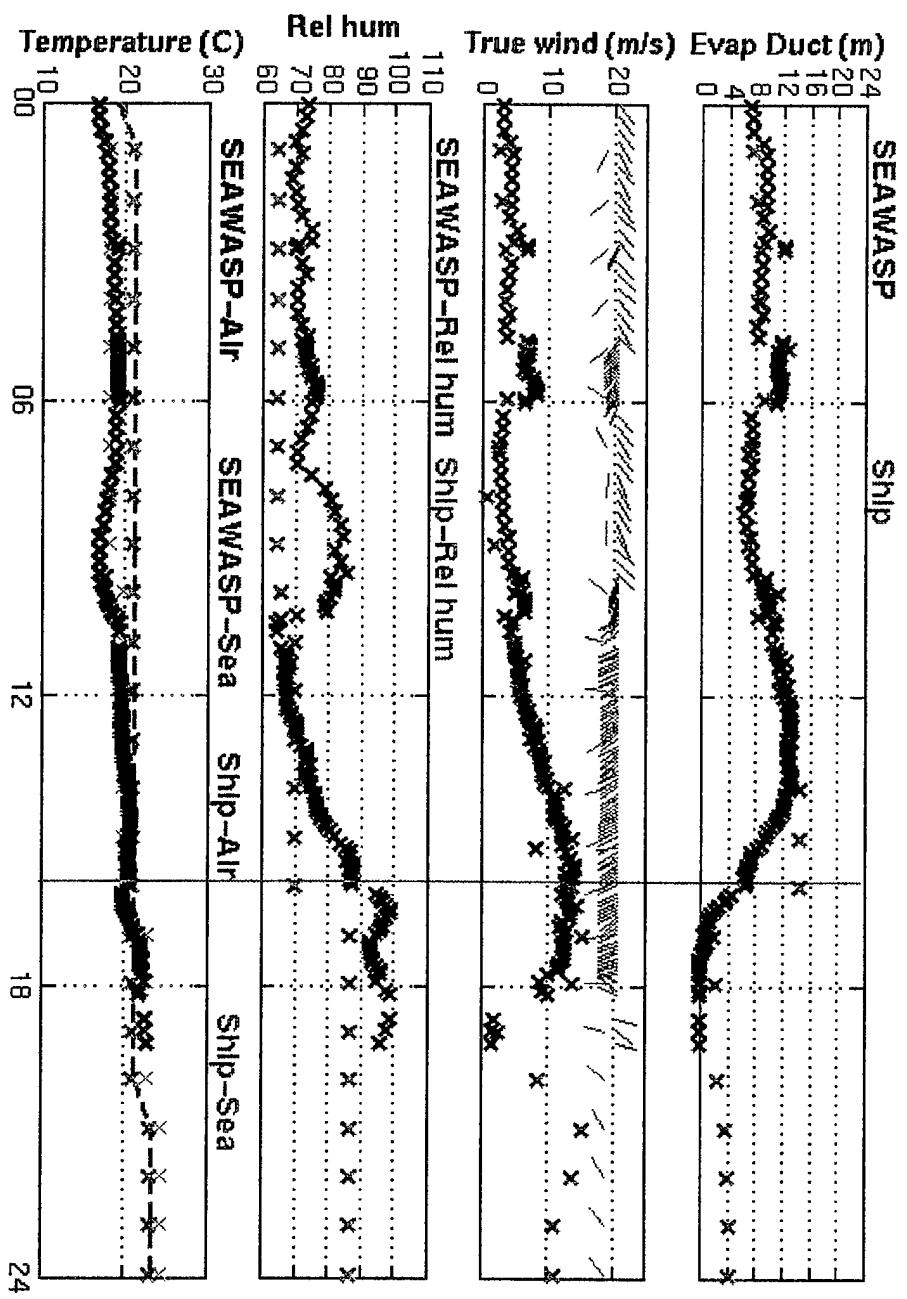
51

Figure 5.9 Time series for 26 July 1997 (41.2N/046.3W) 540nm SE of Newfoundland.
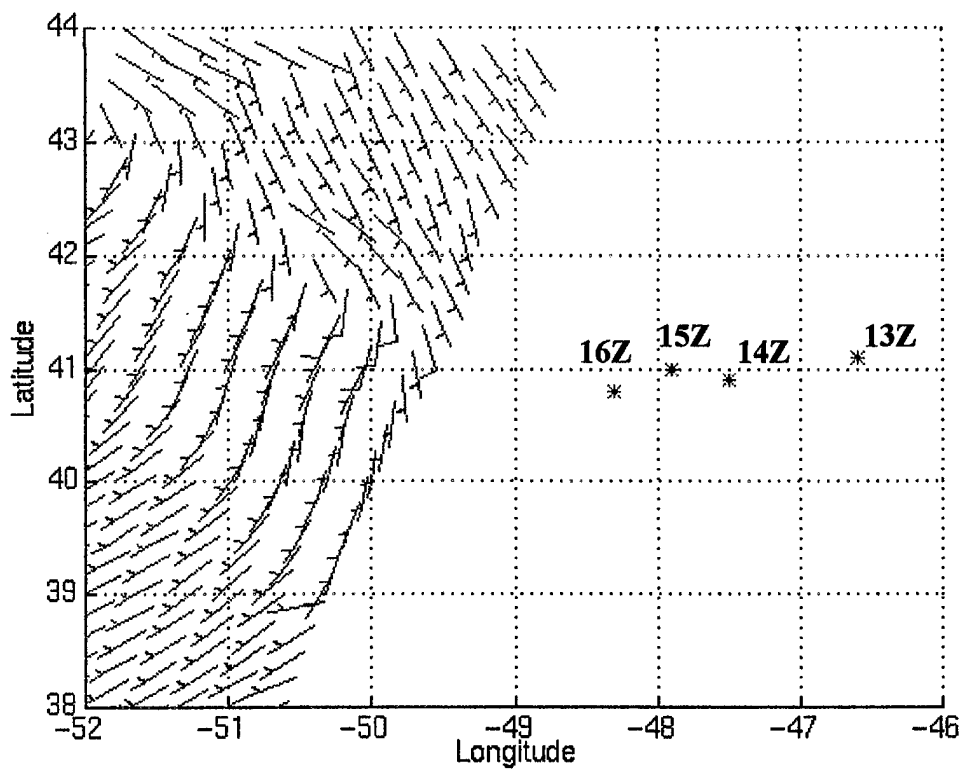
Scatterometer Winds for7/26/97

Figure 5.10 ERS-2 scatterometer winds at 14Z 26 July 1997.

26 JULY 1997 (1555Z)

PROPAGATION LOSS dB

230 200 170 140 110 80

RANGE nm i

0 10 20 30 40 50

LEGEND
SHIP
SEAWASP
SATELLITE
FREE SPACE
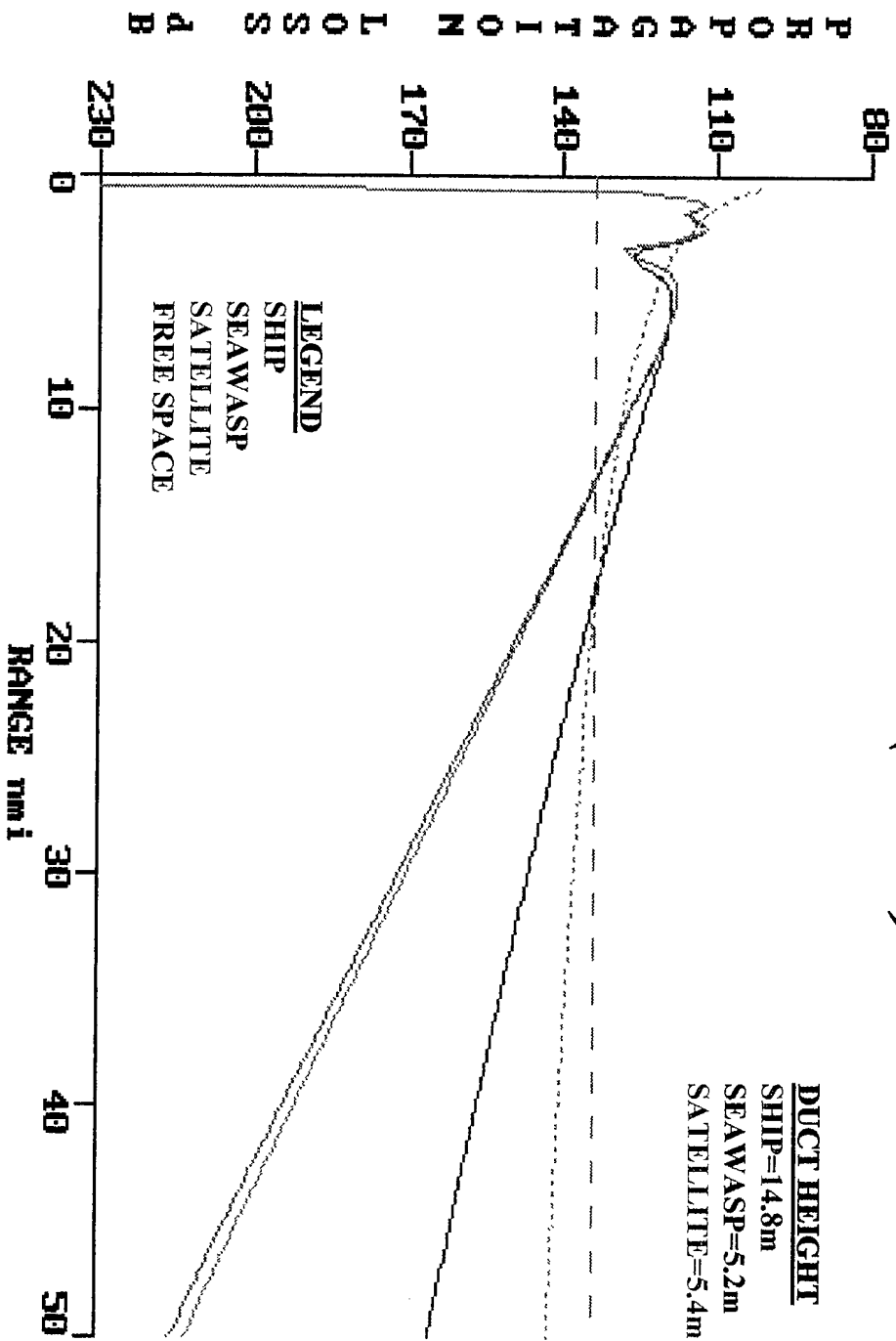
DUCT HEIGHT
SHIP=14.8m
SEAWASP=5.2m
SATELLITE=5.4m

Figure 5.11 Propagation Loss Diagram. Depicts ~6nm difference in detection range between SEAWASP and shipboard measurement systems.
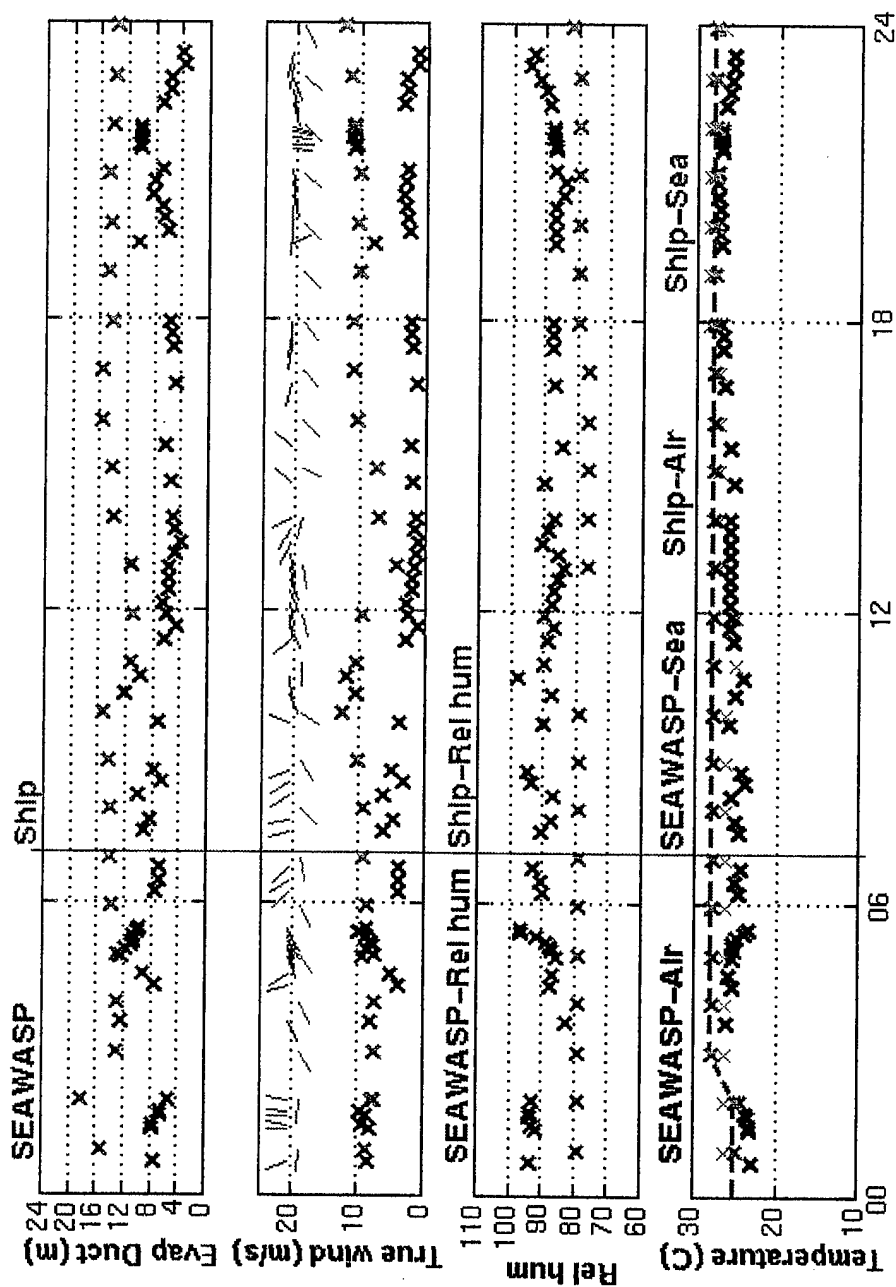
Figure 5.12 Time series for 28 July 1997 (38.5N/064.1W) 360nm ESE of Boston, MA.

55
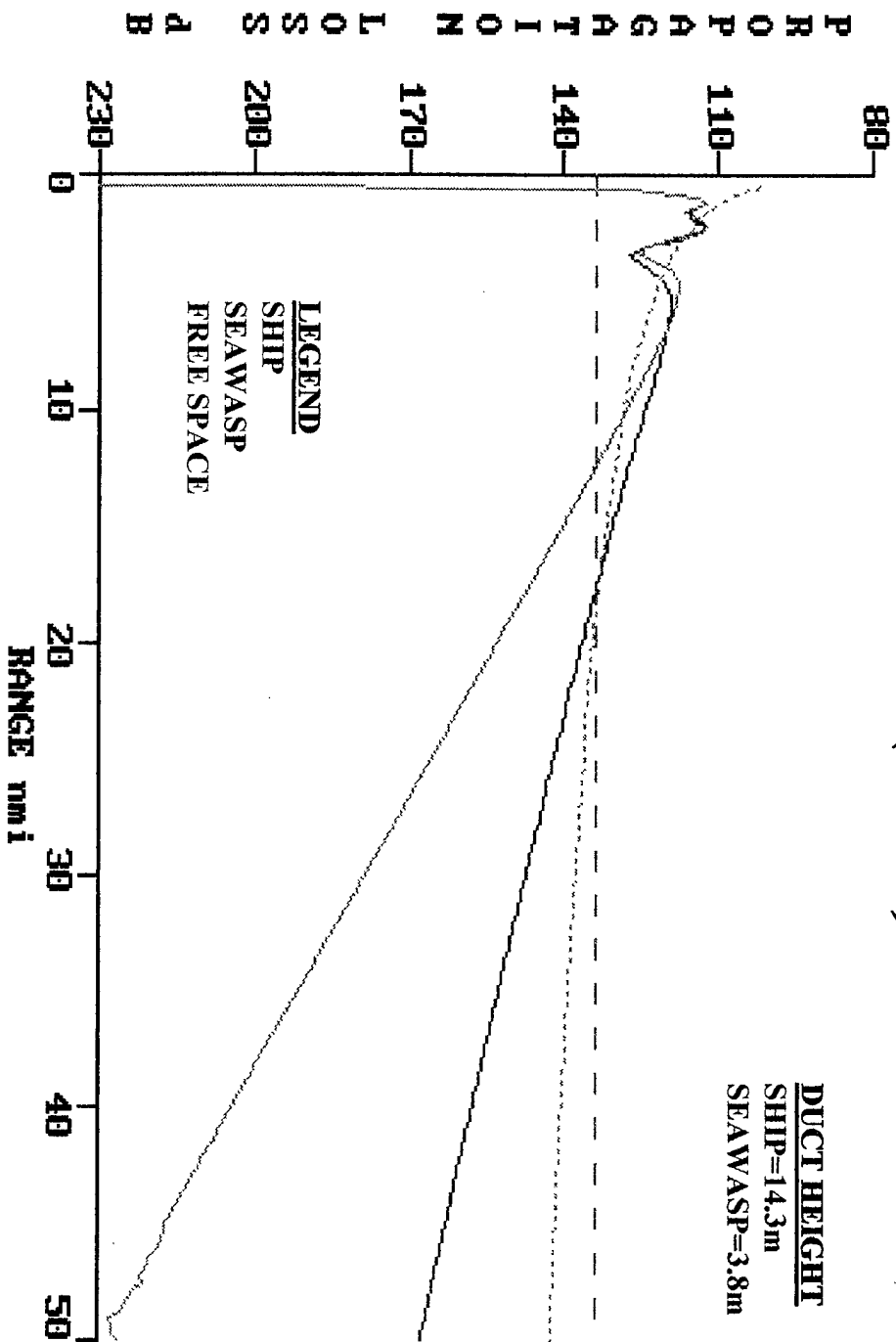
Figure 5.13 Propagation Loss Diagram. Depicts ~6nm difference in detection range.

56

Figure 5.14 Time series for 29 July 1997 (37.2N/073.5W) 150nm NE of Norfolk, VA.

Scatterometer Winds for 7/29/97
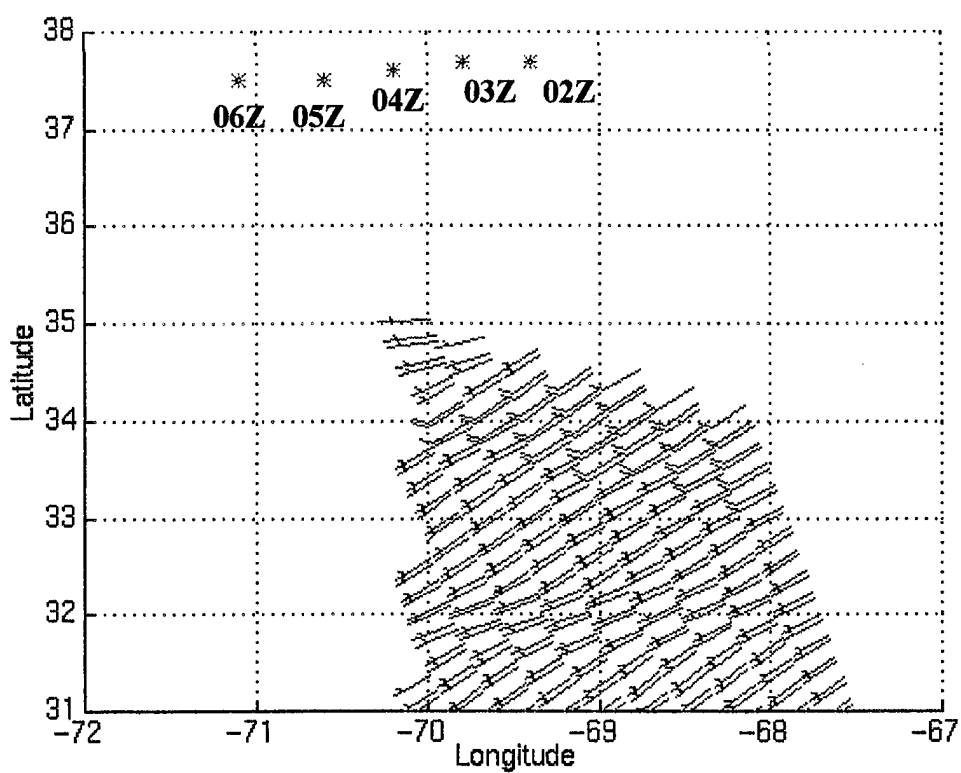
Figure 5.15 ERS-2 scatterometer winds at 03Z 29 July 1997.

58

29 JULY 1997 (0555Z)
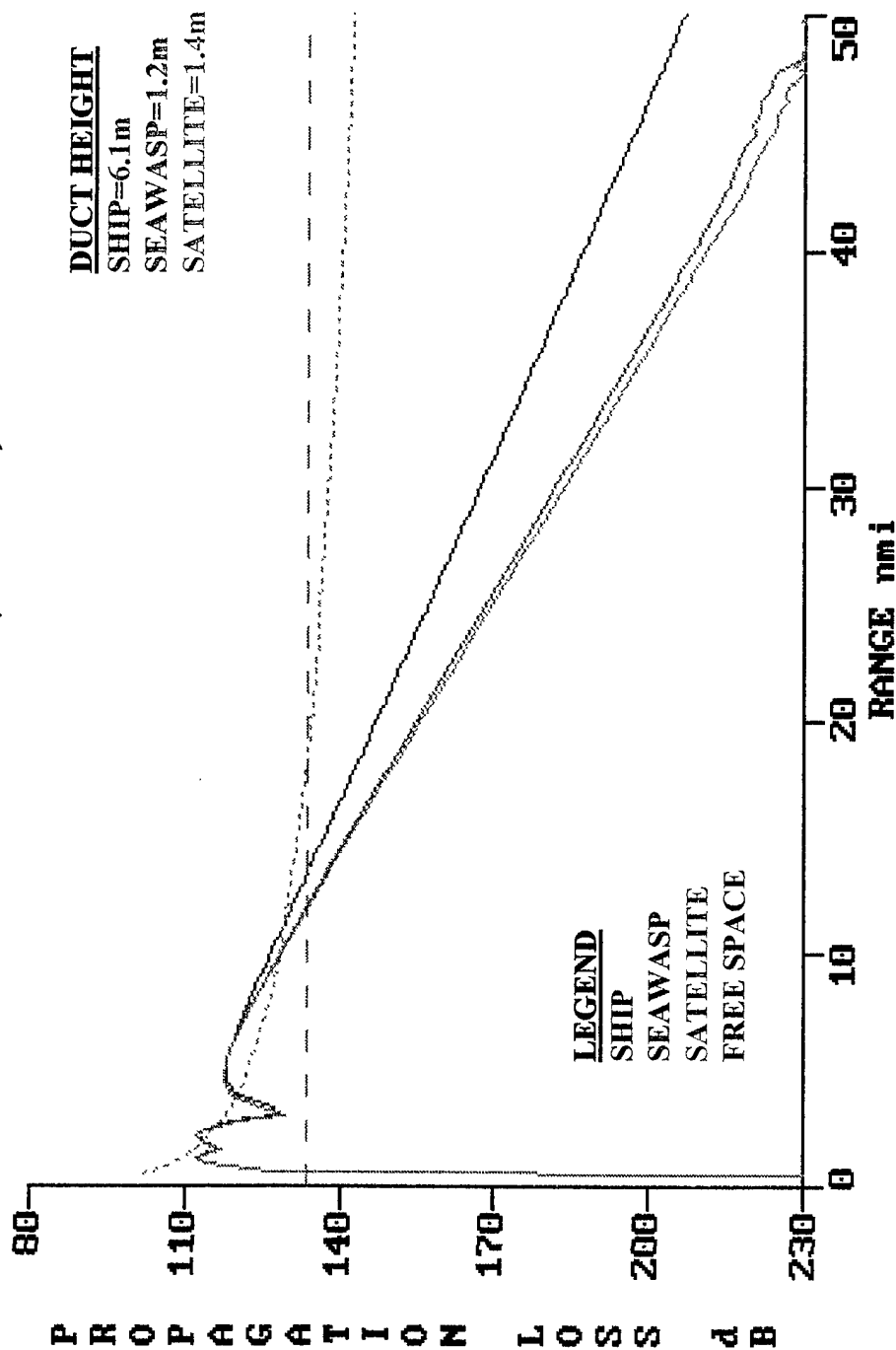
Figure 5.16 Propagation Loss Diagram. Depicts ~2nm difference in detection range between SEAWASP and shipboard measurement systems.
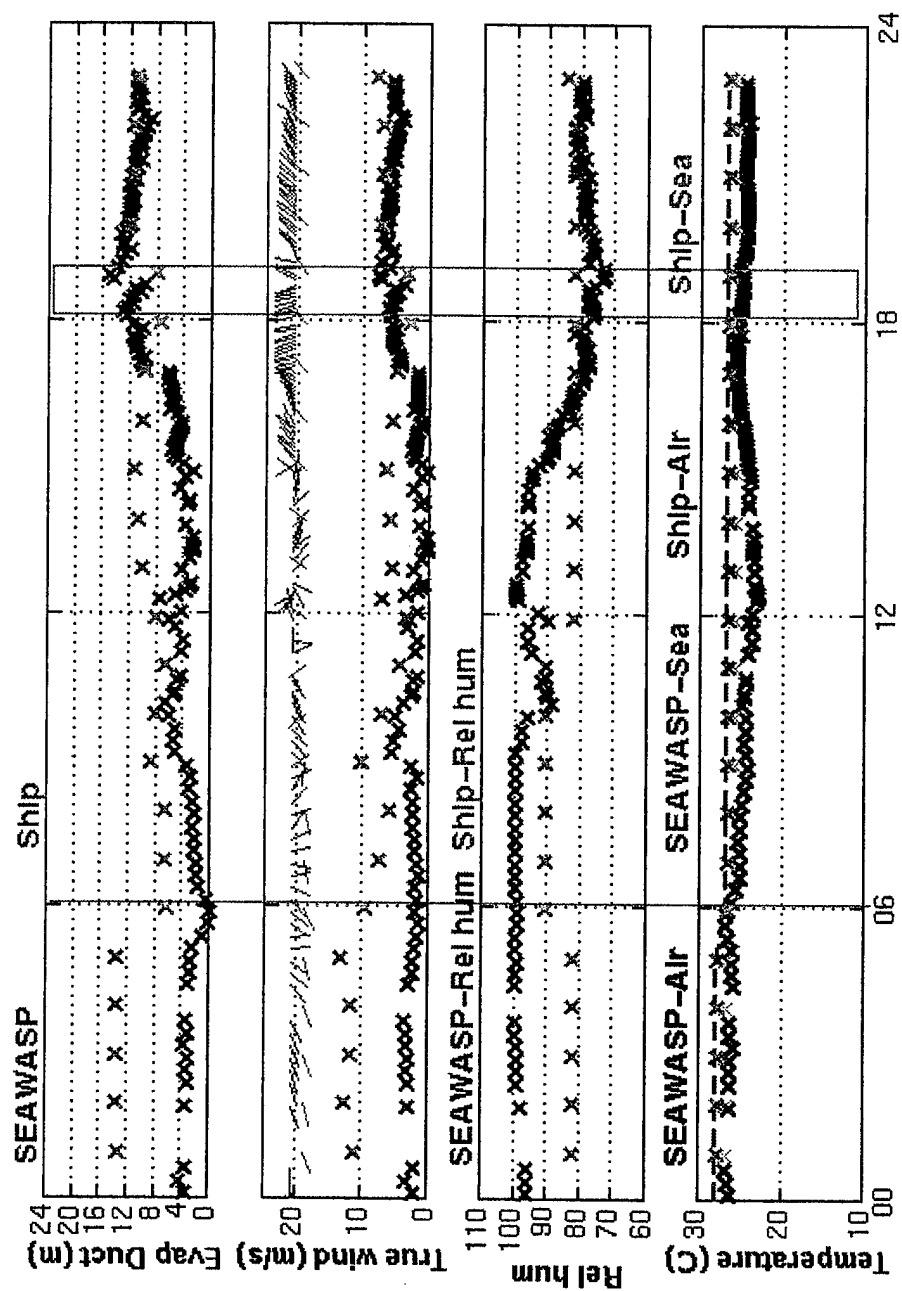
29 July 1997 (1755-1855Z)

P
R
O
P
A
G
A
T
I
O
N

L
O
S
S

d
B

80
110
140
170
200
230

0   10   20   30   40   50

RANGE nm i

DUCT HEIGHT
SHIP(1755Z)=7.6m
SHIP(1855Z)=8.2m
SEAWASP(1753Z)=11.7m
SEAWASP(1808Z)=13.1m
SEAWASP(1843Z)=9.9m
SEAWASP(1853Z)=15.2m

Figure 5.17 Propagation Loss Diagram. Depicts detection ranges due to variability of duct heights during one hour time period.

VI. CONCLUSION

Monitoring increases and decreases in detection time due to changing evaporation duct conditions is critical for naval units deciding whether to engage a threat or operate further from shore. Through an accurate understanding of the existing evaporation duct conditions, radar propagation ranges can be better calculated and used.
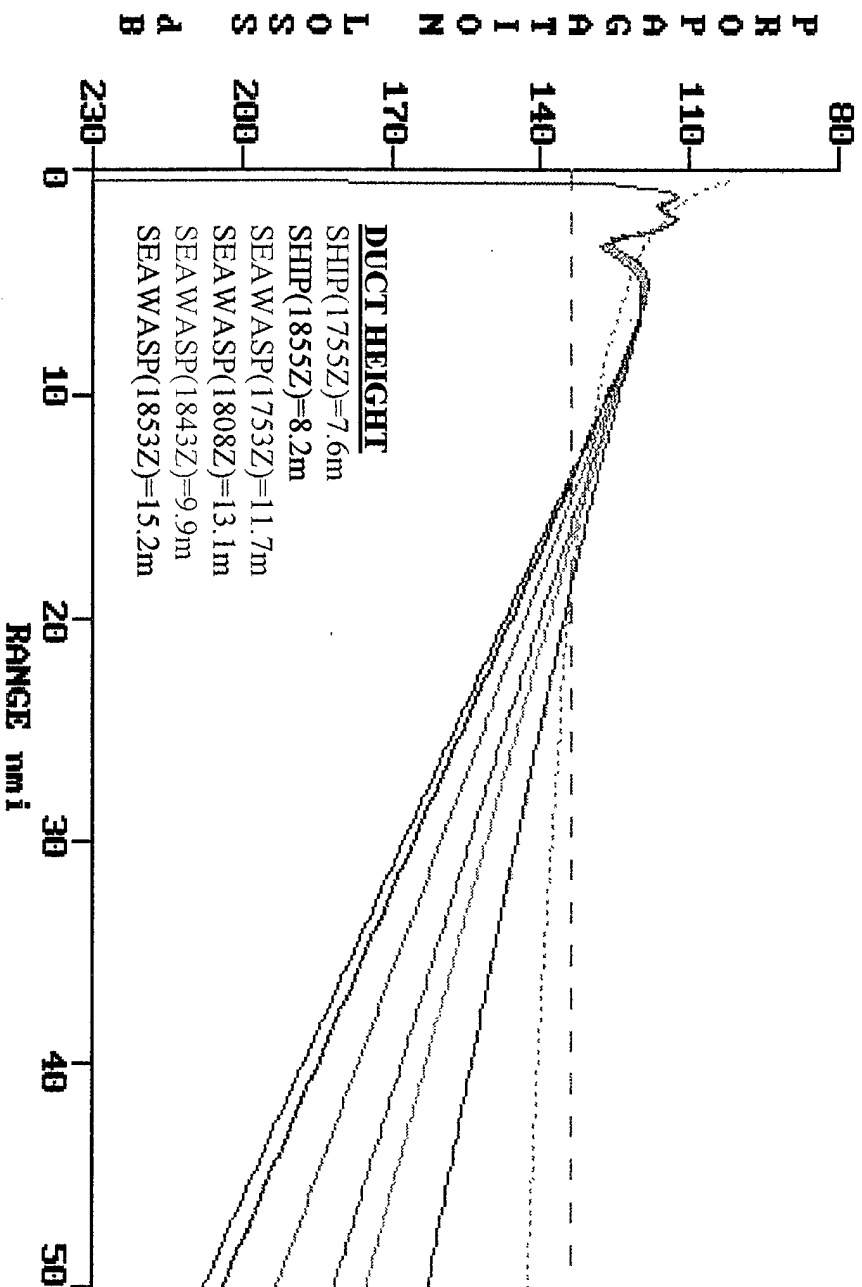
This thesis evaluated SEAWASP, an automated system, designed solely for this purpose. The SEAWASP system was evaluated on a basis of data collected over a two month cruise aboard two AEGIS class cruisers. It was left unattended throughout the cruise as the ships departed Norfolk, VA and transited the North Atlantic to the Baltic Sea and back during the summer of 1997.

Throughout the cruise, SEAWASP provided continuous and accurate measurement of the atmospheric parameters used in calculating the evaporation duct, except for sea surface temperature. The IR sensor used by SEAWASP in determining sea surface temperature was not reliable. Therefore, the ship's recorded sea surface temperature, as measured at the ship's intake, was used in all calculations for this thesis for comparison purposes. While this measurement of sea surface temperature is known to be inaccurate, it was used because it was the only measurement available.

The comparison of an automated and continuous system against hourly observations from ships personnel was interesting. SEAWASP's more accurate and timely measurement of the parameters affecting evaporation duct conditions provided a significant increase in awareness of the ever-changing evaporation duct conditions

surrounding a ship. This capability is critical to the warfare commander when evaporation duct conditions are translated into radar propagation loss curves which depict reaction time. Accurate calculation of evaporation duct heights provide more accurate estimates of the ships radar performance and therefore detection capabilities. This study demonstrated the significant difference between SEAWASP and ships predicted radar propagation ranges, by citing various examples throughout the cruise. In conclusion, SEAWASP, providing automated and continuous measurement of the parameters that determine the evaporative duct conditions, has given the Navy a valuable tool in determining the optimal employment of its sophisticated radar and weapon systems to maintain its decisive edge in naval operations.

Further examination considered over the horizon assets for determining conditions that may impact the ducting environment out ahead of the ship. Using scatterometer wind data, the warfare commander can determine if the ducting conditions out ahead of the ship may increase or decrease. This capability is based on the inverse relationship of wind speed with duct height when the air is warmer than the water. This is a start in addressing the use of overhead assets in determining over the horizon electromagnetic propagation effects for shipboard radar and weapon systems. Concept of operations for this approach has to be developed. It is evident that reliance on raw scatterometer data is not enough due to the frequency and location of the satellite footprint. The merging of other data such as mesoscale model predictions with scatterometer data perhaps would be more beneficial.

LIST OF REFERENCE

Babin, S. M.,Young, G. S., and Carton, J.A., 1997: A new model of the oceanic evaporation duct. *Am. Meteor. Soc.*, 36, 193pp.

Clarke, R., 1997: The Environmental Edge, Tactical Oceanography. *Surface Warfare.*, March/April 1997, 27-31pp.

COMSURFWARDEVGRU Tacmemo AZ3010-1-95, AW Planning Guide, Confidential, 24 March 95.

Dalton, J. H., 1994: Forward...From the Sea, Library of Congress no. VA58.4053, 1994, 10pp.

Fairall, C. W., Bradley, E.F., Rogers, D.P., Edson, J.B., and Young, G.S., 1996: Bulk parameterization of air-sea fluxes for Tropical Ocean-Global Atmospheric Coupled-Ocean Atmospheric Response Experiment. *J. Geophys. Res.*, 101, 3747-3762pp.

Fairall, C. W., Davidson, K.L., Schacher, G.E., and Houlihan, T.M., 1978: Evaporation duct height measurements in the Mid-Atlantic. Naval Postgraduate School., Monterey, CA.

Hitney, H. V., 1995: Radio Physics Optics (RPO) version 1.15 User's Guide. Naval Command, Control and Ocean Surveillance Center, RDT&E Division, San Diego, CA.

Konstanzer, G. C., 1996: SEAWASP: A prototype system for shipboard assessment based on in situ environmental measurements. Johns Hopkins University Applied Physics Laboratory, Laurel, MD.

Lockheed Martin Corp, 1996: AEGIS Combat System Environmental Studies Report. Lockheed Martin Corp., Moorestown, NJ.

Monin, A. S., and A. M. Obukhov, 1954; Basic laws of turbulent mixing in the atmosphere near the ground. *Tr. Akad. Nauk. SSSR Geofz. Inst.*, 24(5), 635-644pp.

Patterson, W. L.,1988: Effective use of the electromagnetic products of TESS and IREPS, Naval Oceans Systems Center, Technical Document 1369, 138pp.

Patterson, W.L. and Hitney, H.V., 1992: Radio physical optic CSCI software documents, Naval Command Control and Ocean Surveillance Center RDT&E division, Technical Document 2403, 318pp.

Patterson, W. L., Hattan, C.P., Lindem, G.E., Hitney, H.V., Anderson, K.D., and Barrios, A.E., 1994: Engineer's Refractive Effects Prediction system (EREPS), Technical Document 2648 Naval Command, Control and Ocean Surveillance Center, RDT&E Division, San Diego, CA.

SEAWASP User Guide, 1997, Johns Hopkins University Applied Physics Laboratory, Laurel, MD.

INITIAL DISTRIBUTION LIST

No. Copies

1. Defense Technical Information Center..2
   8725 John J. Kingman Rd., STE 0944
   Ft. Belvoir, VA 22060-6218

2. Dudley Knox Library...2
   Naval Postgraduate School
   411 Dyer Rd.
   Monterey, CA 93943-5101

3. Commander...1
   Naval Meteorology and Oceanography Command
   Stennis Space Center, MS 39529-5000

4. Chief of Naval Research..1
   800 North Quincy St.
   Arlington, VA 22217

5. Johns Hopkins University...1
   Applied Physics Laboratory
   Laurel Rd.
   Laurel, MD 20723-6099
   Attn: John Rowland

6. AEGIS Program Manager...1
   PMS 400 B30AD
   Arlington, VA 22242-5186

7. Professor K. Davidson..2
   Meteorology Department, Code MR/DS
   Naval Postgraduate School
   Monterey, CA 93943-5002

8. Professor C. Wash..1
   Chairman,Meteorology Department, Code MR/WX
   Naval Postgraduate School
   Monterey, CA 93943-5002